Reservoir Potential of Lower Nari Sandstones (Early Oligocene) In Southern Indus Basin and Indus Offshore*

Syed Amir Mahmud[1] and Shamim Ahmed Sheikh[2]

Search and Discovery Article #50582 (2012)**
Posted March 31, 2012

*Adapted from article prepared, presented, and distributed as part of the Technical Program at SPE/PAPG Annual Technical Conference, Islamabad, Pakistan, November 17-18, 2009

[1]Weatherford Oil Tool Middle East Ltd. (amirmahmud@gmail.com)
[2]Department of Geology, University of Karachi-Pakistan

Abstract

As the need and hunt for new energy resources continues, petroleum geologists keep searching for unexplored hydrocarbon reservoirs. Areas which were supposed not to be economical in the past are being re-evaluated. In this connection studies are under way throughout the world.

In this study sandstones of Lower Nari Formation (early Oligocene) were analyzed. Several outcrop samples were collected from onshore areas and analyzed for environmental assessment and resulting potential reservoir characters. The analyses included detailed petrography, measurement of porosity and permeability, and Scanning Electron Microscopy (SEM) with EDS application.

The sandstones of Lower Nari are classified as quartz arenites. The studies revealed that these horizons were deposited in a shallow-marine environment within the domain of the upper shelf, associated with a passive margin (trailing edge). These sandstones contain fair to good porosity and poor to fair permeability, thus depicting a potential reservoir rock. The facies distribution of Nari Formation suggests that the most prospective target for hydrocarbon exploration may exist in the offshore and adjoining onshore areas, which have sufficient overburden for the generation of hydrocarbon within the probable source, which might be interbedded horizons of Nari shales and underlying Eocene shales of Kirthar Formation. Hydrocarbon shows have also been observed in several onshore and off shore wells (Dabbo Creek 1, Karachi Well 1, etc.) More intense studies in this regard should be done and the offshore Indus area should be re-evaluated with emphasis on Lower Nari as a potential reservoir for hydrocarbons.

Introduction

To meet the growing demand of oil and gas reserves, petroleum geologists keep searching for unexplored hydrocarbon targets. In Southern Indus, besides other horizons, Nari Formation of Oligocene age is a potential reservoir target, as hydrocarbon shows have been observed in several onshore and off shore wells (Raza et al., 1990). According to Quadri (1982) and Quadra and Shuaib (1986), Nari Formation has been encountered in many onshore and offshore wells in and around Karachi. The sandstone of Nari Formation has been targeted for reservoir potentials in the offshore Indus Basin; shales and packstones of Nari are considered to have good source potential. Lower Indus Basin is located just south of Sukkur Rift (Figure 1). It comprises Thar Platform, Karachi Trough, Kirthar Foredeep, and Kirther Fold Belt. The platform and trough extend into the offshore Indus. The Southern Indus Basin is bounded by the Indian Shield to the east and the marginal zone of the Indian Plate to the west. Its southward extension is confined by offshore Murray Ridge-Oven Fracture plate boundary.

Tectonic Setting

The Indian Plate was separated from Australia during the Middle Cretaceous and began to drift northward towards Eurasian Plate. The Indian Plate also has rotated counter-clockwise with respect to the geomagnetic pole. The initial collision between the Indian and Eurasian plates took place at the end of Eocene, with the northeastern margin of the Indian Plate docking first into the Eurasian Plate and pivoting the western margin up against the Afghan Plate in a shear motion. Indian Plate is still penetrating into the Eurasian Plate with a velocity of 4.5 cm/yr and rotating slowly counter-clockwise (Sella et al., 2002). The rotation and translation results in left-lateral transform slip in Balouchistan at approximately 4.2 cm/yr and right lateral-transform slip in Indo-Burma Ranges at 5.5 cm/yr. (Bilham, 2004). Full-scale collision during the Oligocene resulted in a second orogenic pulse in the Himalayas and caused the uplift of many areas in the east and south. Marine sediments were restricted to a narrow but still rapidly subsiding trough in the Kirthar area. The southern Indus area is distinguished from much of the rest of the Pakistan by its continued marginal-sag basin development (Raza, 2004).

The Offshore Indus is the southern extension of Southern Indus Basin and consists of approximately 2000 sq km area between 23° and 25°N latitude and 66° and 68°E longitude. This includes the southern portion of Karachi Trough and extends 100-200 km from shore (Kadri, 1995).

Stratigraphy

The oldest rocks encountered in the southern Indus Basin are of Triassic age (Jhat Pat and Nabisar wells). Central and Southern Indus Basins were undivided until Lower/Middle Cretaceous when Khairpur-Jacobabad High became a prominent positive feature. This is indicated by homogeneous lithologies of Chiltan Limestone (Jurrasic) and Sembar Formation (Lower Cretaceous) across the high. Sand facies of Goru Formation (Lower-Middle Cretaceous) also extend into the Kandhkot and Giandari area. This is also substantiated by the Jhat Pat and Khairpur wells located on the high. In Khairpur 2 well, significant amount of Lower Cretaceous and Paleocene is missing, while in Jhat Pat 1, the whole Cretaceous and Paleocene are absent with Eocene directly overlying Chiltan Limestone (Jurrasic). Paleocene facies south of the high are quite different from those in the north and are dominated by clastic sediments derived from the positive areas (Khairpur-Jacobabad High and Nabisar Arc) (Kadri, 1995).

The stratigraphy on outcrop of southern Indus Basin ranges from Paleocene to Recent (Figure 2). In Karachi Embayment the Oligocene is represented by Nari Formation, which consists of sandstones and shales with subordinate limestones and minor conglomerates. The lower contact of Nari Formation is conformable and gradational with Kirthar Formation of Eocene age in most areas of exposure, while in Hydrabad Anticlinorium (Kirthar Province), it is unconformable with Laki, Gazij, and Kirthar formations (Hunting Survey Corporation, 1961). The upper contact is conformable with Gaj Formation of Miocence age. Nari Formation is considered the equivalent of basal Nal Limestone of Kirthar area and Chittarwatta Formation of Central Indus Basin (Kazmi and M.Q., 1997). In western Balochistan the equivalent rocks of Nari Formation are Kojak Shale (lower part), and are of flysch facies (Farshori, 1972).

Nari Formation is widely distributed in Lower Sindh, including the offshore and Balochistan Province, in areas within and around the southern fold belt between Karachi and Quetta (Figure 3). It has a thickness of 1400m at its type section; i.e., the Gaj River in Kirthar Range, Dadu, Sindh (latitude 26^{o}56'12", longitude 67^{o}10'10"). Whereas it has a thickness of 1045m-1820m in the Khirthar Province, 150m-300m in Sulaiman Province, 200m in Quetta and 600m at Nal in the Axial Belt (Iqbal and Shah, 1980). Nari Formation has also been encountered in many wells; in Karachi-2 well drilled in Karachi depression the thickness was found to be 1798m (Raza et al., 1990).

Nari Formation on the basis of faunal evidence has been placed in Oligocene to early Miocene (Rupelian to early Aquitanian age) (36.6 My. - 21 My.) (Iqbal and Shah, 1980).

Nari Formation is divided into two parts on the basis of fauna and lithology. The lower part was deposited entirely under marine and the upper part under partly marine and partly fluvial conditions (Farshori, 1972). In the area around Karachi, Nari Formation is divided into four members (Figure 4); namely, Tobo, Hab, PirMangho, and Orangi by Geological Survey of Pakistan (Quraishi et al., 2001).

Tobo member is the basal part of Nari Formation in Pir -Mangho area, Karachi. It consists of alternating sandy limestone, sandstone, and shale. Characteristically, it has grey to light brown sandstone, yellowish sandy shale (yellowish green to brown), and dark brown medium-bedded limestone. It is exposed in the core of Pir Mangho Anticline (Field photo # 1).

Material and Methods

In Pir Mangho area, north of Karachi metropolis, several outcrop samples of Lower Nari Formation (Tobo Member) were collected from the exposed core of Pir Mangho Anticline. The samples were analysed for petrography under polarizing microscope. Photomicrographs of thin sections were taken using computerized Wild MPS 46 Photoautomat, wildLeitz mounted on Leitz laborlux 12 POLS. For core analysis small plugs were extracted from the samples using drill press and analyzed for porosity and permeability using steady stat permeameter and Heise-Gauge porosity meter, respectively. Grain density was also calculated. Selected samples were analyzed under scanning electron microscope; spot, line, and elemental mapping were done through Energy Dispersive X-ray analysis System (EDS) (JED 2300 Analysis station).

Results

Petrography

The petrographic studies of the sandstone samples revealed that mostly it is medium to fine-grained, angular to sub angular to rounded with well sorted grains. Calcareous and ferruginous cements are present. Quartz grains dominate the composition, with microcline, plagioclase feldspars, micas, and lithic fragments present in minor quantities. Few fossils and broken fossils fragments are also present. The detail of the samples is as follows.

Sample # 02

A calcareous quartz arenite, fine- to very fine-grained, angular to subrounded. and very well sorted. Carbonate and siliceous (meniscus) cement is present. Quartz is dominant (99%) (PM # 1), with very small amount of polycrystalline quartz, muscovite and plagioclase feldspar. Few of the grains have healed fractures.

Sample # 04

- grained, angular to sub rounded and well sorted. Calcareous (intragranular), siliceous (meniscus) and ferruginous cement is present. Quartz is dominant with a very small amount of polycrystalline quartz, microcline, muscovite, plagioclase (PM # 2), and volcanic rock fragments are also present (PM # 3). A number of grains have healed fractures (PM # 4). Considerable amounts of fossil fragments are also present; these fossils seem to be squeezed, bent and broken under pressure.

Sample # 05

A calcareous, ferruginous quartz arenite, medium- to fine-grained, angular to subrounded and moderately sorted. It is bimodal. Siderite, calcitic, and iron oxide cements with gradation are present. Quartz is dominant (99%); few flakes of muscovite and grains of polycrystalline quartz are also present.

Sample # 06

A calcareous, ferruginous quartz arenite, medium- to fine-grained, angular to subrounded and well sorted. Sideritic cement is present (PM # 05). Quartz is dominant (99%) with few grains of muscovite, plagioclase (PM # 06), and rock fragments (PM # 07). Most of the grains have healed fractures; sideritic rhombs (PM # 08) are also fractured.

Sample # 07

A calcareous, ferruginous quartz arenite, medium- to fine-grained, angular to subrounded and moderately sorted. Sideritic cement is present. It is bimodal (PM # 09). Quartz is dominant (99%) with few grains of microcline (PM # 10) and volcanic rock fragments (PM # 11). Most of the grains are fractured.

Sample # 8L

A calcareous quartz arenite, medium- to fine-grained, angular to rounded and well sorted. Carbonate (intergranular and meniscus) cement is present (PM # 12). Quartz is dominant (99%) with few grains of microcline, plagioclase, muscovite (PM # 13, 14), polycrystalline quartz, and volcanic rock fragments. Broken calcareous fossil fragments are also present. (*Lepidocyclina* (PM # 15) *Lepidocyclina polylepidine* (PM # 16), *Bermudezina* (PM # 17). Many of the grains are highly fractured at places. Iron oxide is present and fills the chambers of fossils (PM # 18).

Sample # 8U

A calcareous, ferruginous quartz arenite, fine-grained, angular to rounded and well sorted. It contains sideritic and calcitic cement (sideritic cement is replaced by calcite cement). Quartz is dominant (99%) with few grains of polycrystalline quartz (PM # 19) and igneous rock fragments. Many of the grains are fractured. Zoned crystals of dolomite/siderite are also present (PM # 20, 21).

Sample # 9L

A calcareous, ferruginous quartz arenite, fine-grained, angular to subrounded and well sorted. Sideritic and calcitic cement is present. Quartz is dominant with a very small amount of polycrystalline quartz.

Sample # 9U

A calcareous, ferruginous quartz arenite, fine-grained, angular to subangular and well sorted. Sideritic and calcitic cement is present. Quartz is dominant.

Core Analysis

Small plugs were extracted from the samples as per the details given in Material and Methods. The plugs were analyzed for porosity, permeability and grain density which yielded the following results (Table. 1).

Scanning Electron Microscopy

A scanning electron microscope with chemical analytical capability using energy dispersive analysis (SEM/EDX) is useful in mineralogy as a source of morphological and compositional data on individual mineral grains. Some of the grains of quartz, feldspars, and clay minerals are very tiny and hardly distinguished under ordinary polarizing microscope, and they need SEM (Friedman and Sanders, 1978).

Samples having higher porosity and permeability were analyzed using SEM (JED 2300 Analysis Station), the following analysis were undertaken:
I. Spot Analysis
II. Line Analysis
III Elemental Mapping

Discussion

The petrographic studies of the sandstone samples reveal that mostly they are medium- to fine-grained, angular through subangular to rounded, and well sorted. They contain calcareous and ferruginous cements. Quartz grains dominate the composition, with microcline, plagioclase feldspars, micas, and lithic fragments present in minor quantities. Few fossils and their fragments are also present. The rock is classified as orthoquartzite (Folk, 1968), and quartz arenite (McBride, 1963; Dott, 1964). The mineralogical composition and texture of the samples suggest that most of the sandstones are texturally and mineralogicaly mature.

With more than 95 % of the grains are quartz and less than 5 % are feldspar, etc., deriving this from a granite source containing more then 70 % feldspar requires prolonged weathering and abrasive action. Therefore, it requires stable tectonic conditions with plutonic source and humid climate (Folk, 1968).

The presence of highly shattered and fractured quartz grains shows the action of tectonics; it might also be an indicator of metamorphosed origin of quartz. Whereas the studies reveal that these quartz belong to a cratonic interior provenance (Dickinson, 1985) (Figure 11). Plots on the QFL diagram of (Yerino and Mayard, 1984) (Figure12) suggests that the center of deposition was associated with a passive margin (trailing edge).

The cement is mostly ferruginous, calcareous, and partly siliceous and sideritic. In some samples the calcareous cement has replaced iron cement showing digenetic changes. Digenetic processes (cementation) are much more likely to reduce the porosity of sandstone than to augment it (North, 1985).

The fossils identified include *Lepidocyclina*, *Lepidocyclina polylepideine* and *Bermudezina*. Broken fossil fragment of forams were also observed. The environment in which they lived is interpreted by their occurrence in cyclic deposits that formed during advance and retreat of shallow seas on the continental platform. The forams chiefly lived in a clear, shallow marine environment far from shore. They characterize rock strata formed during maximum marine invasions. They are not present in brackish water, nearshore sediments or closely associated with evaporites (Moore et al., 2004).

The fundamental property of a reservoir rock is its porosity, along with its permeability. Porosity is the percentage of the total pore spaces, whether the pores are connected or not. Permeability is the property of a medium allowing fluids to pass through it (North, 1985). The comparison of the core analysis of the Lower Nari sandstone samples with the standard values (North, 1985) revealed that most of the samples contain fair porosity but very poor permeability whereas one sample (#5) contains good porosity and poor to fair permeability (Figure 10).There are a number of producing fields throughout the world with low permeability values; e.g., Yaodian oil field, China (Feng et al., 2007), Krishna-Godavari Basin, India, (Mahanti et al., 2006), Changqing Yanhewan block, China (Zang et al., 2007), Alderson Member -Hatton Gas Pool, SW Saskatchewan, Canada (Pedersen, 2003), and marine Cretaceous sandstones in Saskatchewan (Simpson and Singh, 1980).

Samples (5, 9L) were analyzed using the SEM technique, which revealed that sample # 5 is fine-grained sandstone. The average size of the grains is ~ 5-15 m. The grains are angular to subangular indicating proximity of provenance. The sorting is poor and has good porosity and interconnecting permeability. The grains exhibit no preferred orientation. The matrix is low in content, which is mostly clay. The present range of magnification (x 2000) does not allow the observation of the morphology of matrix material. The above characters are representative of a good reservoir.

The spot analysis of one selected elongated grain (Figure 6) shows rhombic habit presence of dolomite with some impurities of Si, Al, and K. Probably, it is secondary mineral growth within the void spaces. The presence of Si, Al, and K indicates that the sandstone was slightly arkosic. They became available during weathering. It is inferred that the orthoclase was sourced from granitic rock, which upon alteration formed quartz and clay particles (especially kaolinite). The clay particles occupied interstitial spaces as matrix.

Elemental mapping of spot mineral is illustrated in (Figure 8). Magnesium is nearly evenly distributed throughout in a part of the grain, but Ca is more confined in the left part, indicating that initially it formed as dolomite and later changed into low magnesium calcite, which is stable at normal temperature and pressure. It is interesting to note that Si, Al, and K occupy more in the opposite side (right), indicating that Ca was concentrated in the late phase. Similarly line analysis also indicates dominance of Ca, O, Al, through the line A-B (Figure 7).

The magnification of Sample # 9L is much higher (x 2700), but the resolution is not clear as compared to Sample # 5. It is difficult to classify the rock on the basis of scanned diagram. However, it appears to be siltstone. The average size of the grains is ~10 m. The grains are angular and seem to be platy. There are a number of voids, which are not filled with any primary or secondary mineral.

One small piece (3 m) of subangular grain is present at the upper part of the scanned figure. It has tabular habit, similar to feldspars. The spot analysis of the grain (Figure 9) illustrate Si>Al>O>K, indicating K-feldspar composition of the grain. As described earlier, the rock unit has some unaltered feldspars. Orthoclase is very susceptible to weathering and alters to kaolinite, halloysite, and sericite. Most probably, the grain is microcline, which is low temperature polymorph of Kfeldspar. Microcline is more stable than orthoclase. Laghari (2005) also verified the presence of microcline in the Nagar Parkar igneous complex. Regionally it is the part of NW Indian craton that extends into Pakistan. The craton contains mosaic of reworked Archean basement, Proterozoic fold belt (Aravalli-Delhi) and Upper Proterozoic suites of Malani, Jalore and Siwana (Sinha-Roy et al., 1997). According to Roy and Jhakar (2002), the Malani magmatism is related to Pan-African magmatic events (780-680 Ma).

The different elements show nearly even distribution in microcline. However, Ca and Mg are also present in minor quantities, demonstrating presence of dolomite, either as coating the grain or as an alteration product of some other ferromagnesian mineral.

In Nari Formation some gas shows have been recorded in Dabbo Creek 1 and Karachi well 1 (Raza et al., 1990). According to (Shuaib and Shuaib, 1994), Paleocene, Eocene, Oligocene, and Miocene sandstones/limestones are the primary objectives for hydrocarbon reservoirs in Offshore Indus Basin.

The sandstone reservoirs are distributed in the major part of Southern Indus Basin. The sandstone reservoir facies also exist in the offshore and adjacent onshore areas. The other deposits of sandstone reservoir facies have been developed in the north-south-oriented area in Kirthar depression. The most prospective target for hydrocarbon exploration may exist in the offshore areas, which have sufficient overburden for the generation of hydrocarbon. Apart from the reservoir characters the geochemical analysis of shale samples of Nari Formation in Kirthar Range indicates source-rock potential with TOC 0.86 % and VR=0.94 (Raza et al., 1990).

Conclusions

- The sandstones horizons of Lower Nari Formation are classified as orthoquartzites and quartz arenites.
- The sandstone was deposited in a shallow-marine environment within the domain of the upper shelf, associated with a passive margin (trailing edge).
- The petrographic studies suggest mostly intragranular porosity, with very low amount of fracture porosity.
- The high magnification studies by SEM add to the understanding of mineral composition, cementation, and diagenetic characteristics of Lower Nari Sandstones.
- The porosity and permeability data indicate that sandstones of Lower Nari hold the potential to be a hydrocarbon reservoir.
- The most prospective zone for accumulation of hydrocarbons might be the Indus offshore, as the area is likely to have substantial overburden for generation. The interbedded shale horizons in Nari Formation may act as source rock, as they have shown to be source potential in previous studies.
- It is recommended that the Indus offshore area should be re-evaluated with emphasis on Lower Nari to be studied as potential reservoir horizon.

Acknowledgments

We are thankful to Dr.Nayar Ahsen (Geological Survey of Pakistan) for his support in the preparation of thin sections and Mr.Khalid Muzaffar (Core Lab) for the core analysis.

Selected References

Bilham, R., 2004, Historical studies of earthquakes in India: Annals of Geophysics, p. 1-26.

Dickinson, W.R., 1985, Interpreting provenance relations from detrital modes of sandstones, *in* Zuffa, G.G., ed., Provenance of Arenites: Dordrecht, Netherlands, Reidel Publishing, p. 333-361. `

Dott. R.H. 1964, Wacke, greywacke and matrix - what approach to immature sandstone classification: Journal of Sedimentary Petrology 34 , p. 625-632.

Farshori, M.Z., 1972, The Geology of Sind: Department of Geology, University of Sind, Jamshoro, Sind, India, 81 p.

Feng, J., W. Li, Z. Ouyang, F. Yu, H. Cao, and Y. Zhao, 2007, Characteristics and assessment of Chang 6 sandstone reservoirs in Northern Yaodian Oilfield: Proceedings of The First International Forum on Petroleum Sustainable Development for PhD Candidates.

Folk, R.L., 1968, Petrology of Sedimentary Rocks: Hemphill's Publishers, Austin,Texas, USA, 170 p.

Friedman, G.M., and J.E. Sanders, 1978, Principles of Sedimentology: New York, John Wiley & Sons, New York, USA, 792 p.

Iqbal, M.W.A., and S.M.I. Shah, 1980, A guide to the stratigraphy of Pakistan: Geological Survey of Pakistan, Quetta, Pakistan, v. 53, 37 p.

Kadri, I.B., 1995, Petroleum Geology of Pakistan: Pakistan Petroleum Limited, Karachi, Pakistan, 275 p.

Hunting Survey Corporation (H.S.C), 1961, Reconnaissance geology of part of West Pakistan (Columbo Plan Cooperative Project): Canada Government, Toronto, Canada, 550 p.

Kazmi, A., 1997, Geology and Tectonics of Pakistan: Graphic Publishers, Karachi, Pakistan, 554 p.

Laghari, A., 2005, Petrology of the Nagarparkar granite and associated basic rocks, Thar Desert, Sindh, Pakistan: Ph. D. Thesis, National Center of Excellence in Geology, University of Peshawar, Peshawar, Pakistan, 297 p.

Mahanti, S., A.K. Nayal, A.K. Mathur, and S.R. Anand, 2006, Low permeability Triassic Gondwana reservoirs of Mandapeta Graben, Krishna-Godavari Basin, India: Proceedings of AAPG International Conference 2006 Perth, West Australia, Abstract.

McBride, E.F., 1963, A classification of common sandstones: Journal of Sedimentary Petrology, v. 33/3, p. 664-669.

Moore, R.C., C.G. Lalicker, and A.G. Fisher, 2004, Invertebrate Fossils: CBS Publishers, New Dehli, India, 766 p.

North, F.K., 1985, Petroleum Geology: George Allen & Unwin, Ltd., London, England, 607 p.

Quadri, V.N., 1982, Petroleum and Pakistan offshore: Petroleum Institute of Pakistan, 7 p.

Quadri, V.N., and S.M. Shuaib, 1986, Hydrocarbon prospects of Southern Indus Basin, Pakistan: AAPG Bulletin, v. 70/6, p.730-747.

Quraishi, I.H., S.A.A. Shah, M.A. Tariq, M.S. Khan, S.N. Ahsan, and M.L. Khanzada, 2001, Geological map of Karachi area, Sindh Pakistan: Geological Survey of Pakistan, Map series number 3 .

Raza, A., 2004, Microfacies analysis of Gaj Limestone Cape Monze area, Karachi: Proceedings of PAPG-SPE Annual Technical Conference, Islamabad, p. 485-493.

Raza, H.A, M.S. Ali, and A. Riaz, 1990, Petroleum Geology of Kirthar Sub-Basin and part of Kutch Basin: Pakistan: Journal of Hydrocarbon Research, v. 2/1, p. 29-73.

Roy, A.B., and S.R. Jakhar, 2002, Geology of Rajasthan (Northwest India)Precambrian to Recent: Scientific Publishers, India, 421 p.

Sella, G.F., T.H. Dixon, and A. Mao, 2002, A model for Recent plate velocities from space geodesy: Journal of Geophysical Research, p. 107.

Shuaib, S.M., and S.M.T. Shuaib, 1994, Facies changes and hydrocarbon presence in offshore Indus Basin, Pakistan: Pakistan Journal of Hydrocarbon Research, v. 6/1-2, p. 25-39.

Sinha-Roy, S., G. Malhotra, and M. Mohanty, 1997, Geology of Rajastan: Geological Society of India, 1st edition, 278 p.

Yerino, L.N., and I.B. Mayard, 1984, Petrography of modern marine sands from the Peru-Chile Trench and adjacent areas: Sedimentology, v. 31, p. 83-89.

Zang, Y., N.S. Zang, X.F. Li, J.R. Xiao, H. Liu, and J. Yang, 2007, Changqing Yanhewan block ultra-low-permeability reservoir injection-production method study and optimization: Proceedings of The First International Forum on Petroleum Sustainable Development for PhD Candidates.

Plug	Permeability md	Porosity He %	Grain Density gm/cc
1	0.02	12.46	2.72
5	1.17	17.32	2.73
6	0.02	10.65	2.75
7	0.02	8.70	2.73
8U	0.06	9.10	2.74
8L	0.08	8.58	2.70
9L	0.73	14.16	2.69
11	0.25	10.51	2.70

Table. 1. Result of core analysis.

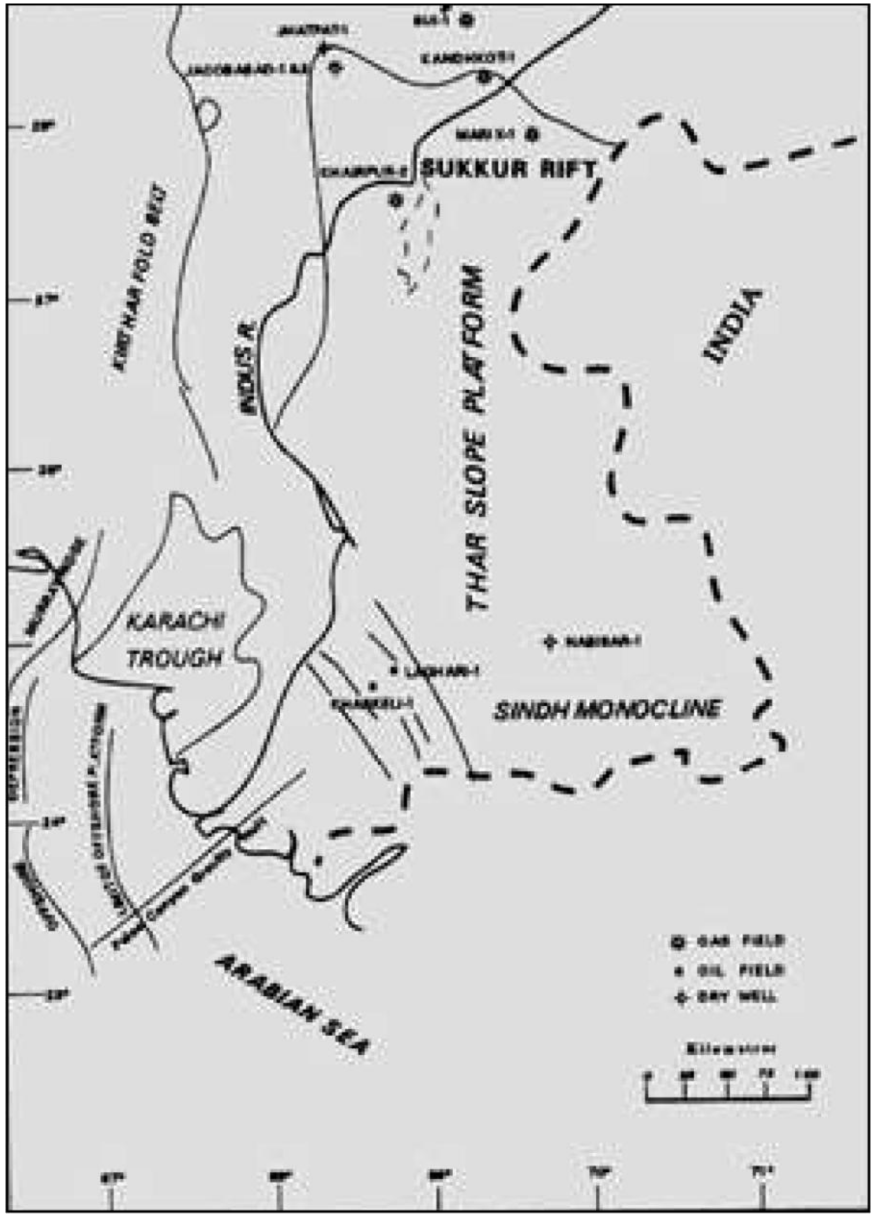

Figure 1. Structural setting of Southern Indus Basin.

ERA	PERIOD		EPOCH	Formation	Description
CENOZOIC	TERTIARY	NEOGENE	Pliocene Pleistocene	MANCHAR	Sandstones and Conglomerate
			Miocene	GAJ	Shale, Sandstone and Limestone
		PALEOGENE	Oligocene	NARI	Shale, Limestone and Sandstone
			Eocene	KIRTHAR	Interbeds of Limestone and Shale with minor marls
				LAKI	Mainly Limestone, Subordinate Marl, Calcareous Shale, Sandstone and laterite
			Paleocene	RANIKOT	Limestone, Sandstone, Shales and coal seams

Figure 2. Stratigraphy (on outcrop) of Southern Indus Basin.

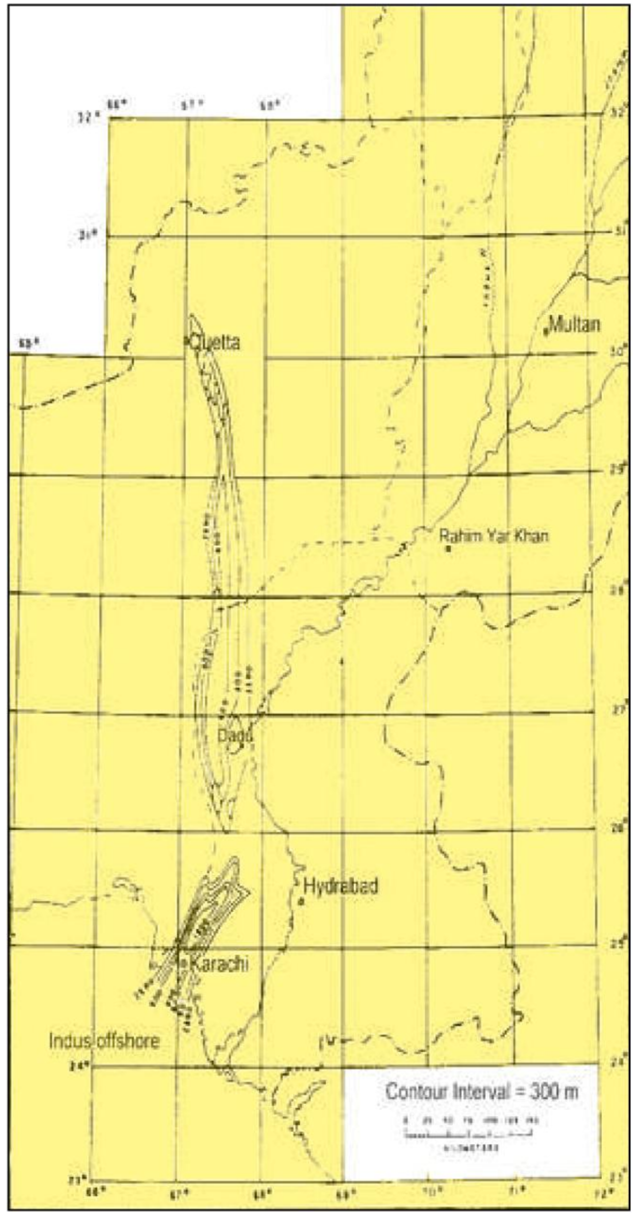

Figure 3. Thickness map of Nari Formation.

STAGE	Formation	Member	Description
BURDIGALIAN AQUITANIAN	GAJ	--	Sandstone, Limestone and subordinate Shale
	NARI	ORANGI	Sandstone with subordinate Clay and Limestone
	NARI	PIR MANGHO	Limestone Clay and Sandstone
CHATTIAN	NARI	HAB	Massive Sandstone with minor Sandy Clay
RUPELIAN	NARI	TOBO	Alternating Sandy Limestone Sandstone and Clays
PRIABONIAN	KIRTHAR	--	Interbeds of Limestone and Shale with minor marls

Figure 4. Internal stratigraphy of Nari Formation.

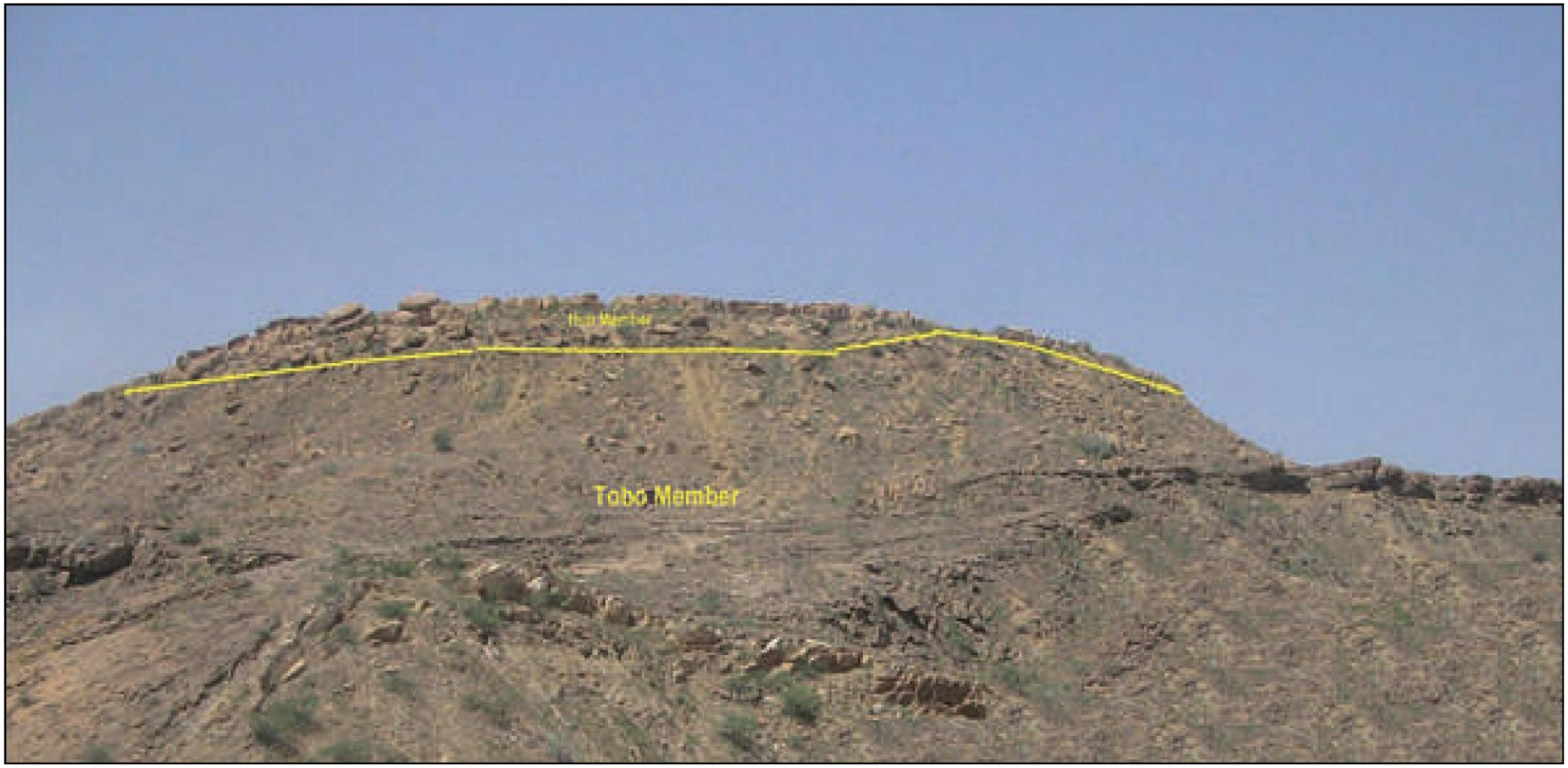

Figure 5 (Field photo # 1). Exposed core of Manghopir Anticline Karachi showing upper conformable contact of Tobo (Lower Nari Formation) with Hub Member. (Looking in plunge direction).

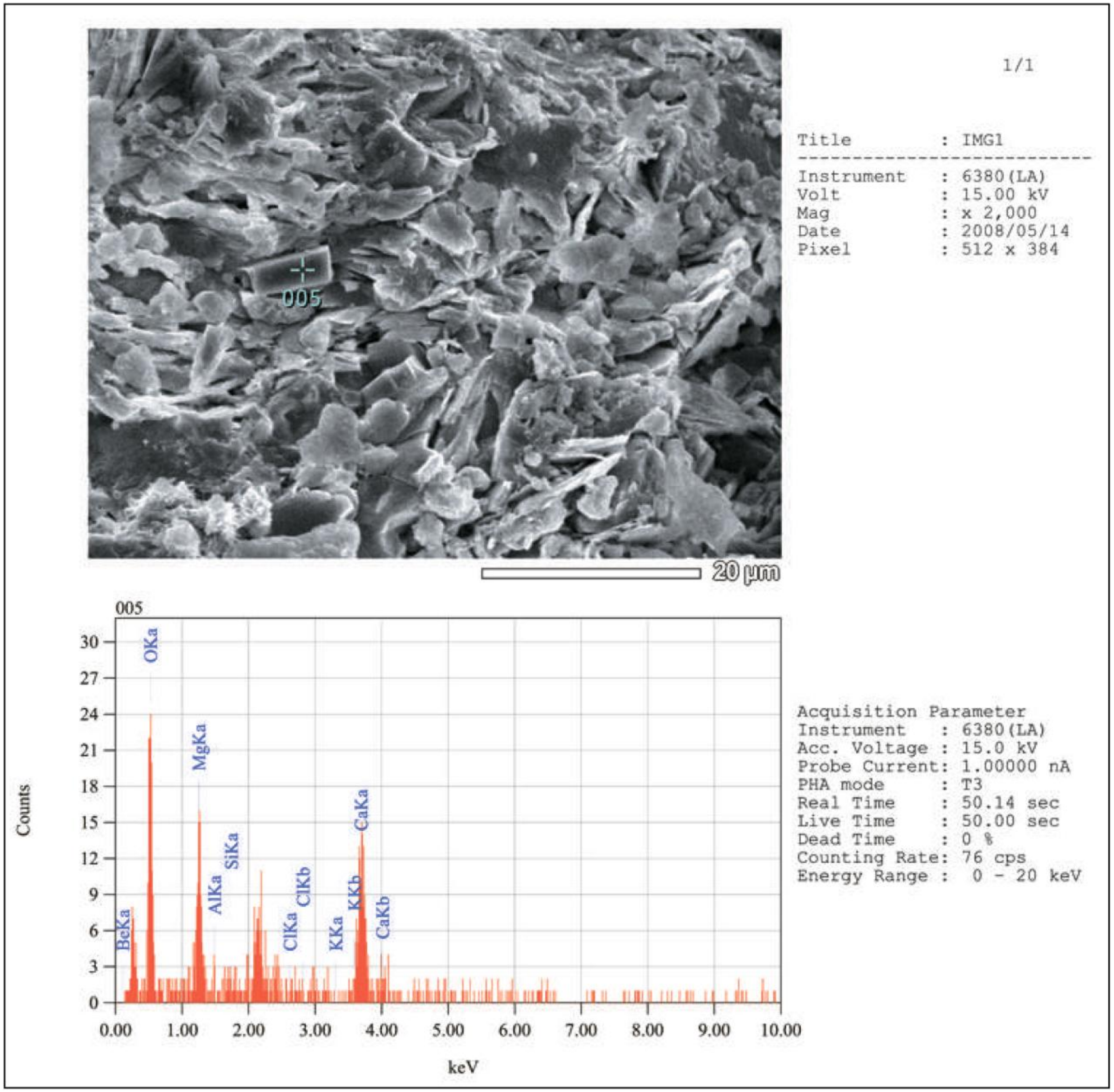

Figure 6. Spot analysis of sample # 05.

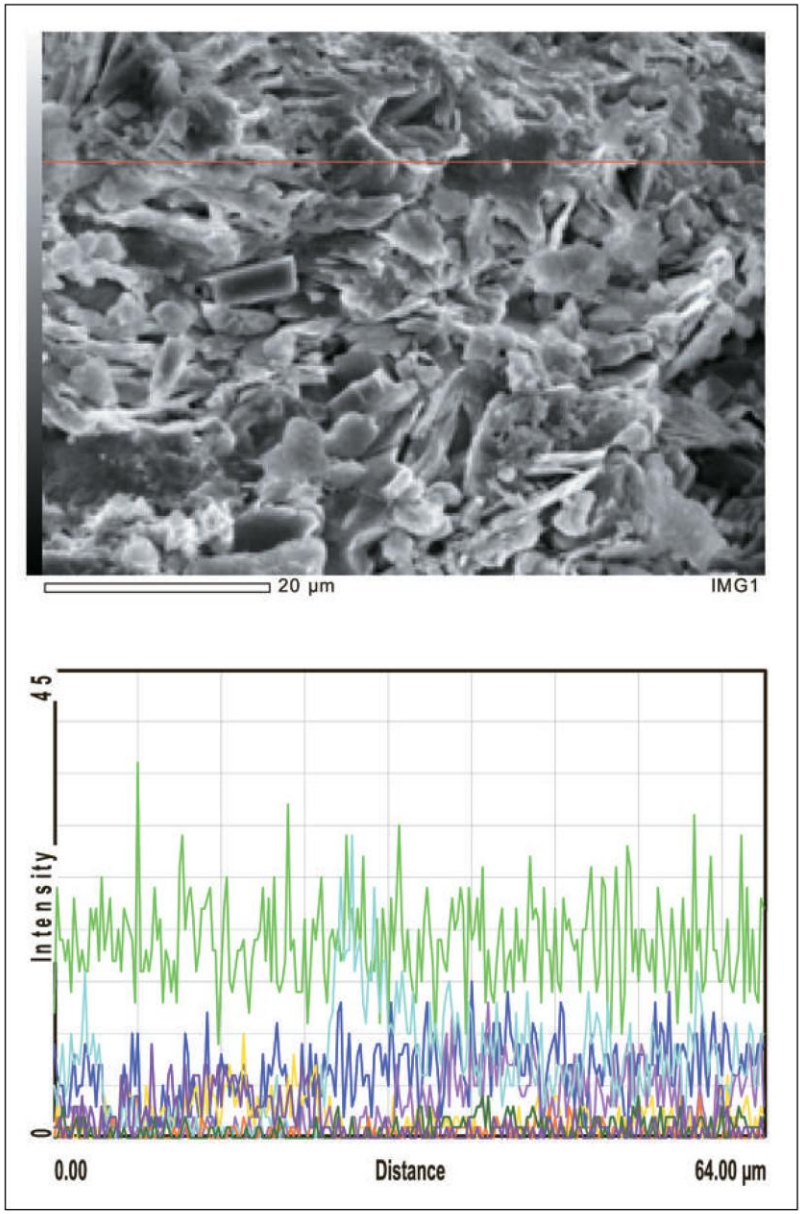

Figure 7. Line analysis of sample # 05.

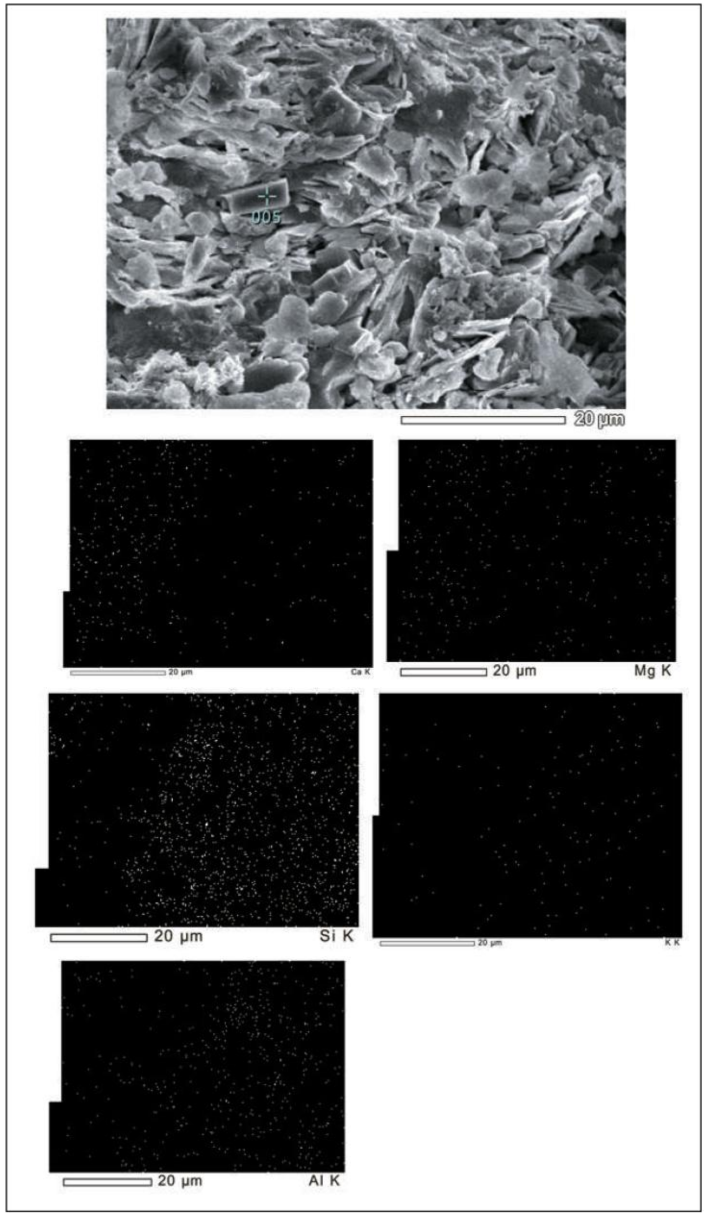

Figure 8. Elemental mapping of sample # 05.

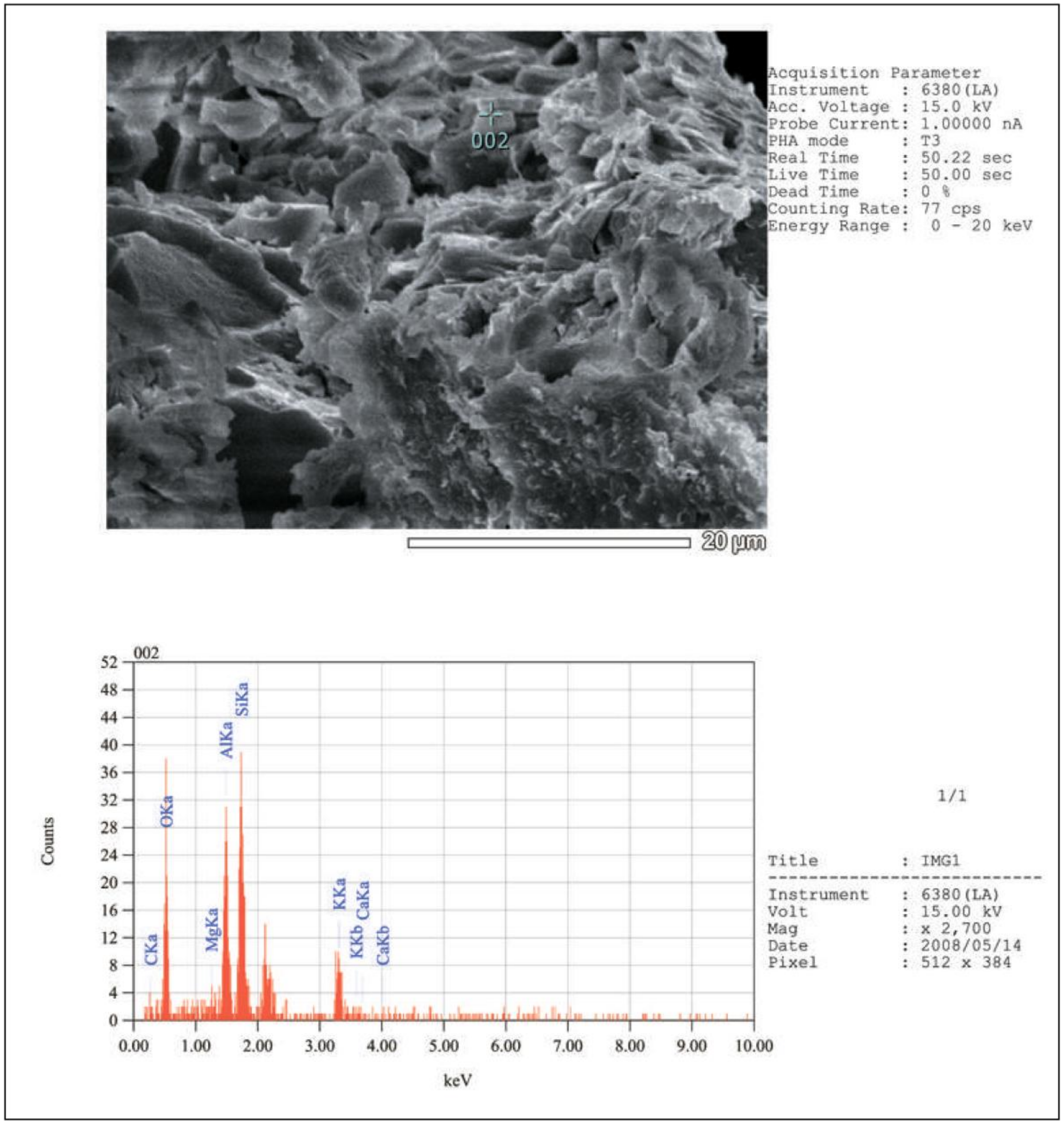

Figure 9. Spot analysis of sample # 9L.

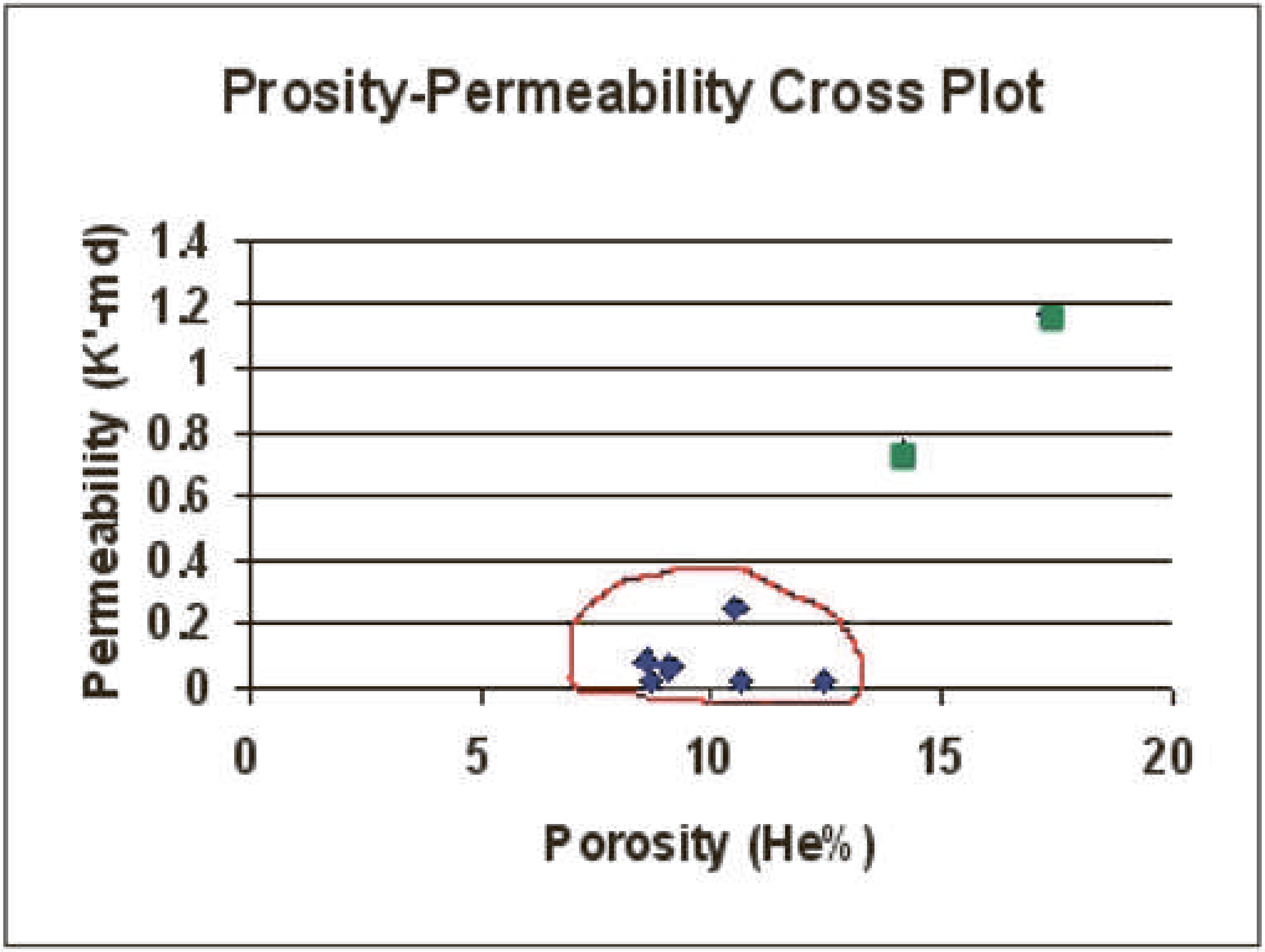

Figure 10. Cross plot of core analysis.

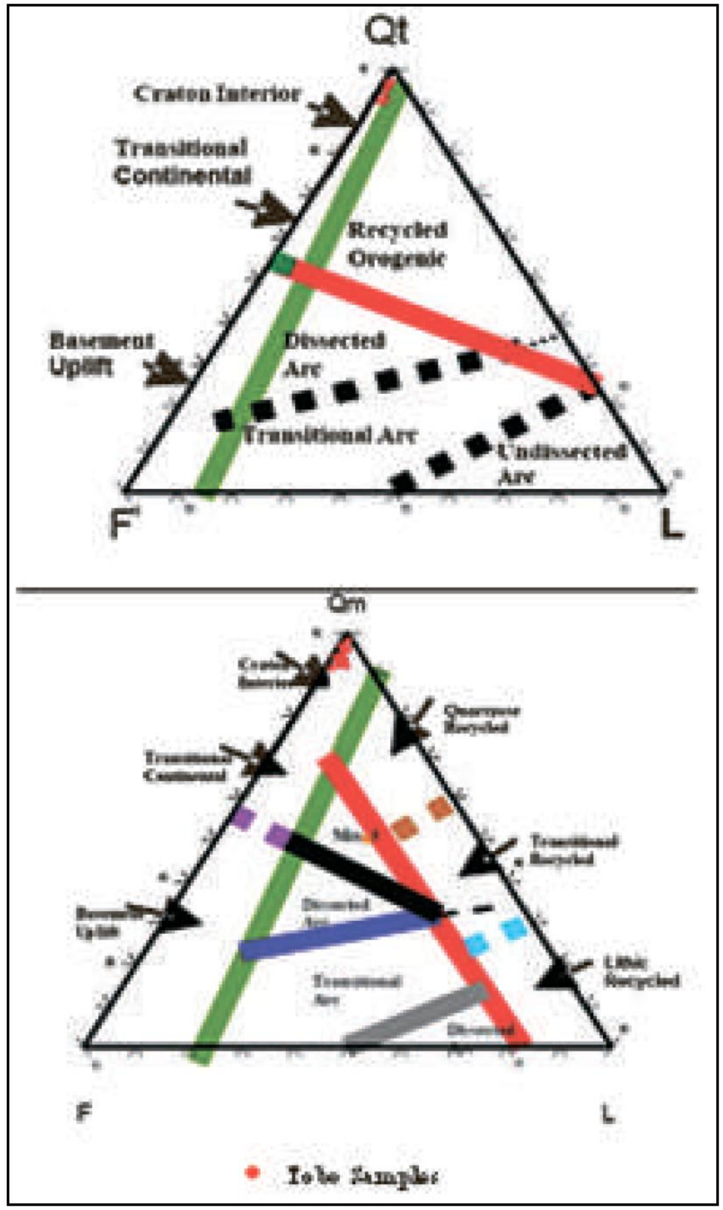

Figure 11. Plots of Lower Nari sandstone samples on QFL diagram showing provenance terrain (Dickinson, 1985).

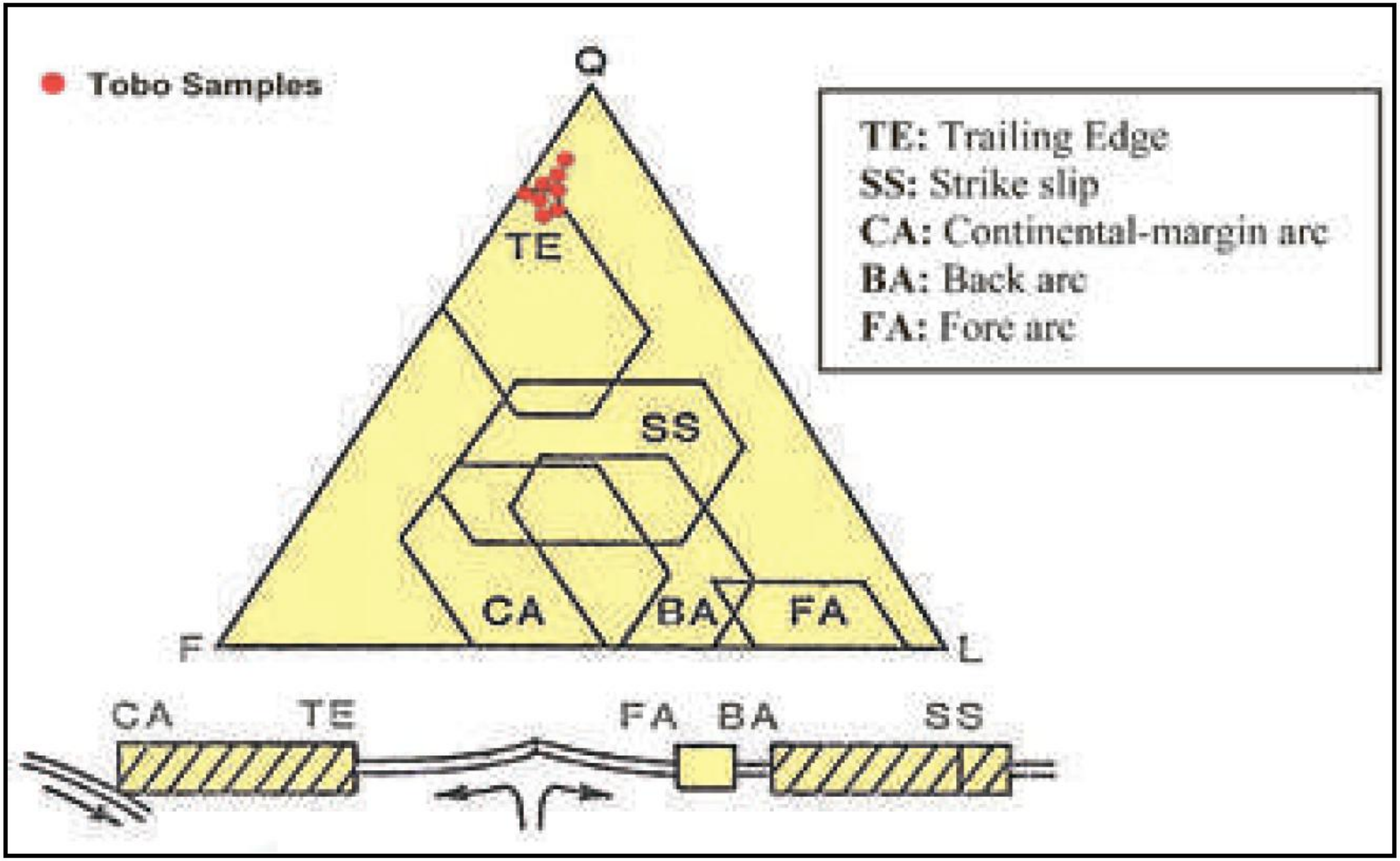

Figure 12. Plots of Lower Nari sandstone samples on triangular diagram showing tectonic setting of the area of deposition (Yerino and Mayard, 1984).

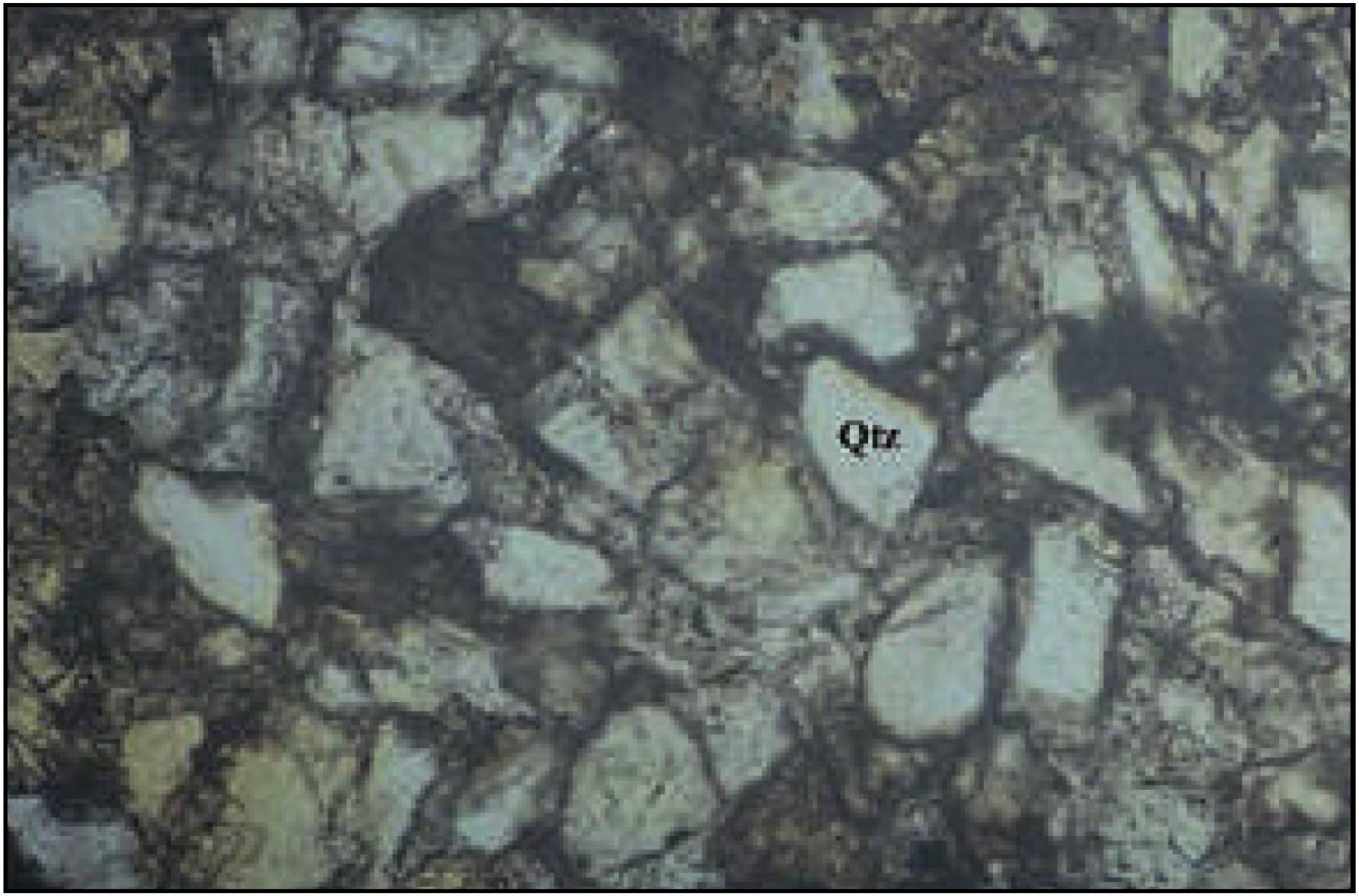

PM # 1. Quartz grains (99 %), Sample No. 02, parallel nicols, 125X.

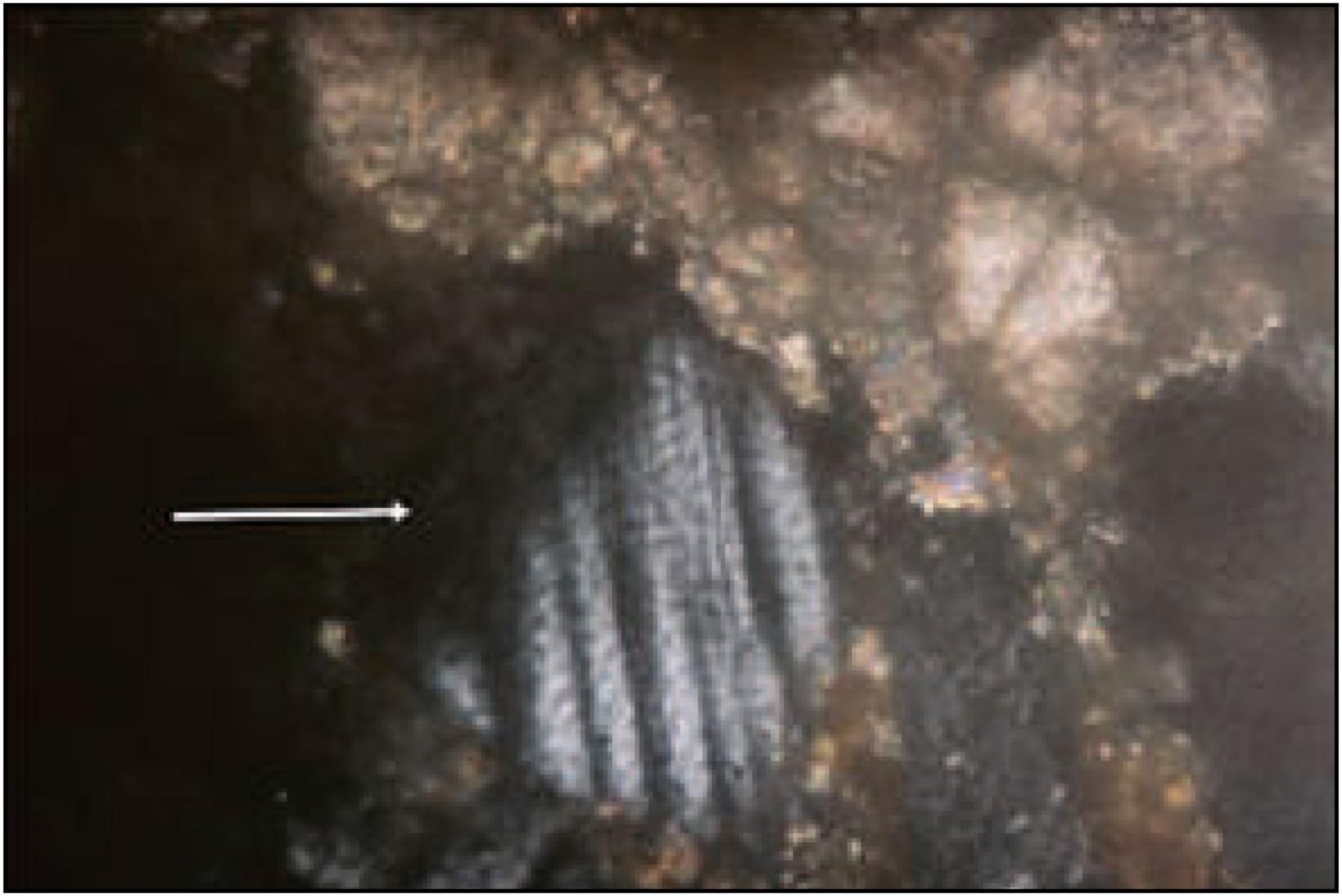

PM # 2. Plagioclase, Sample No. 04, cross nicols, 500X.

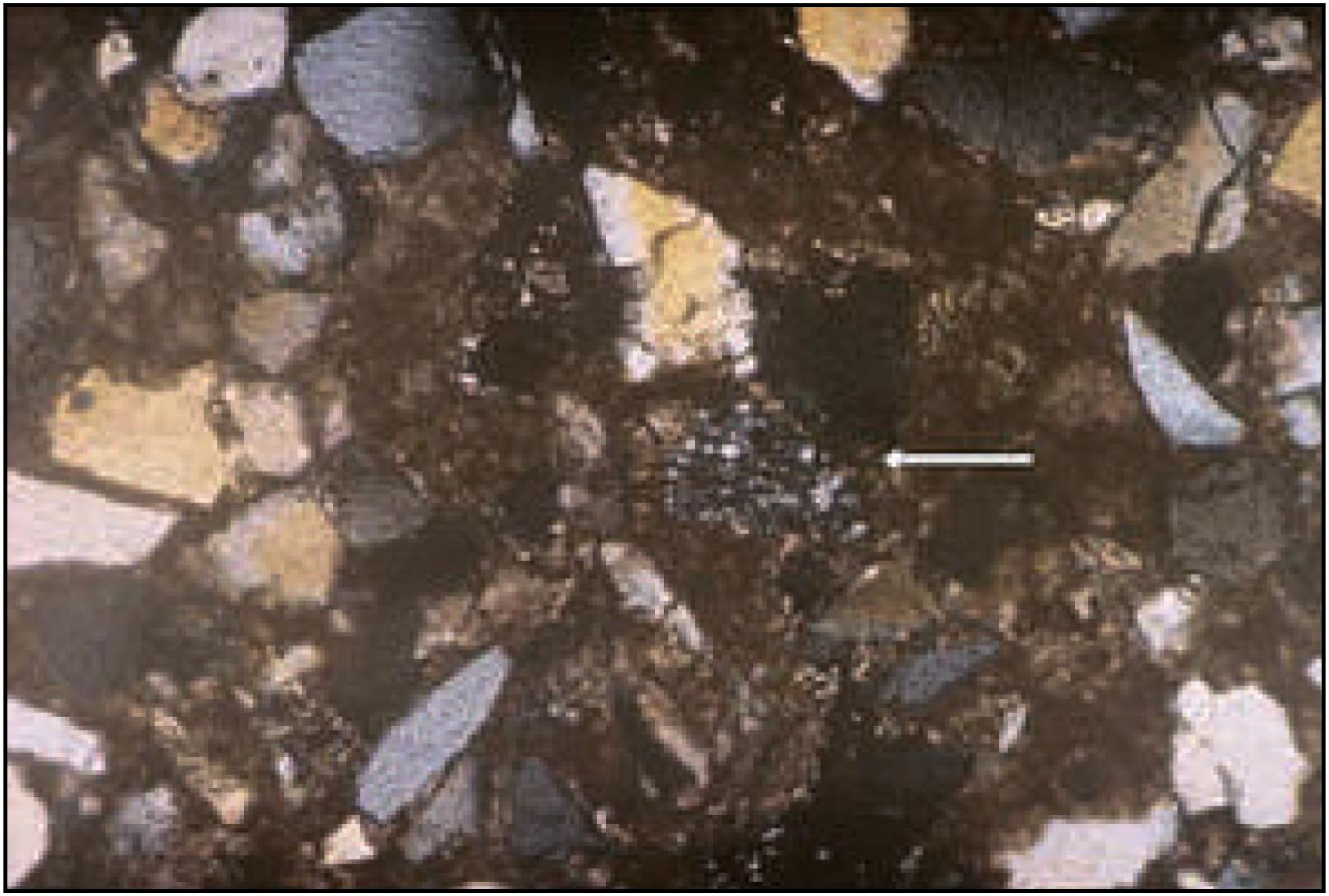

PM # 3. Igneous rock fragment, Sample No. 04, cross nicols, 125X.

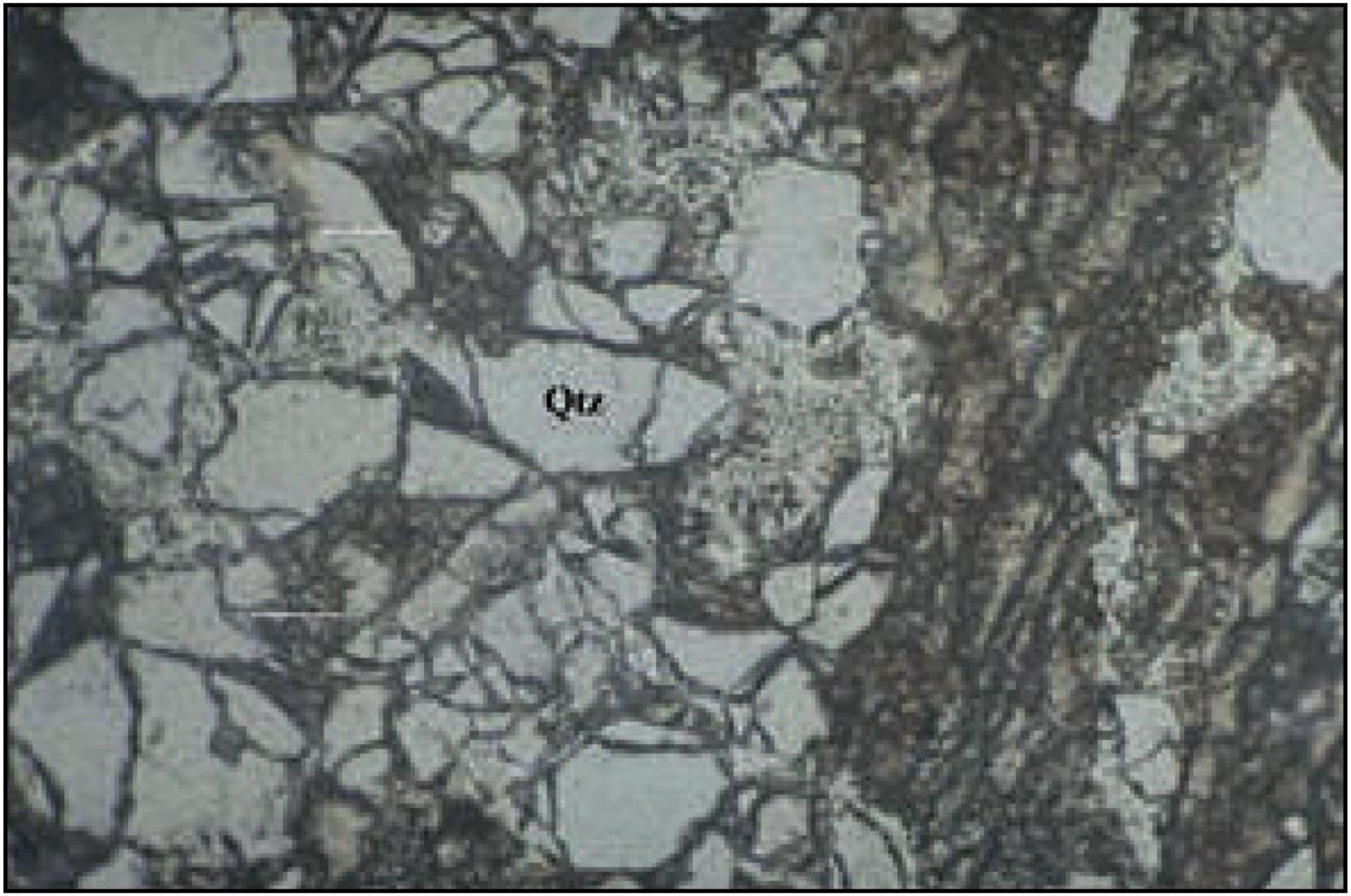

PM # 4. Healed fracture in quartz grains, Sample No. 04, parallel nicols, 125X.

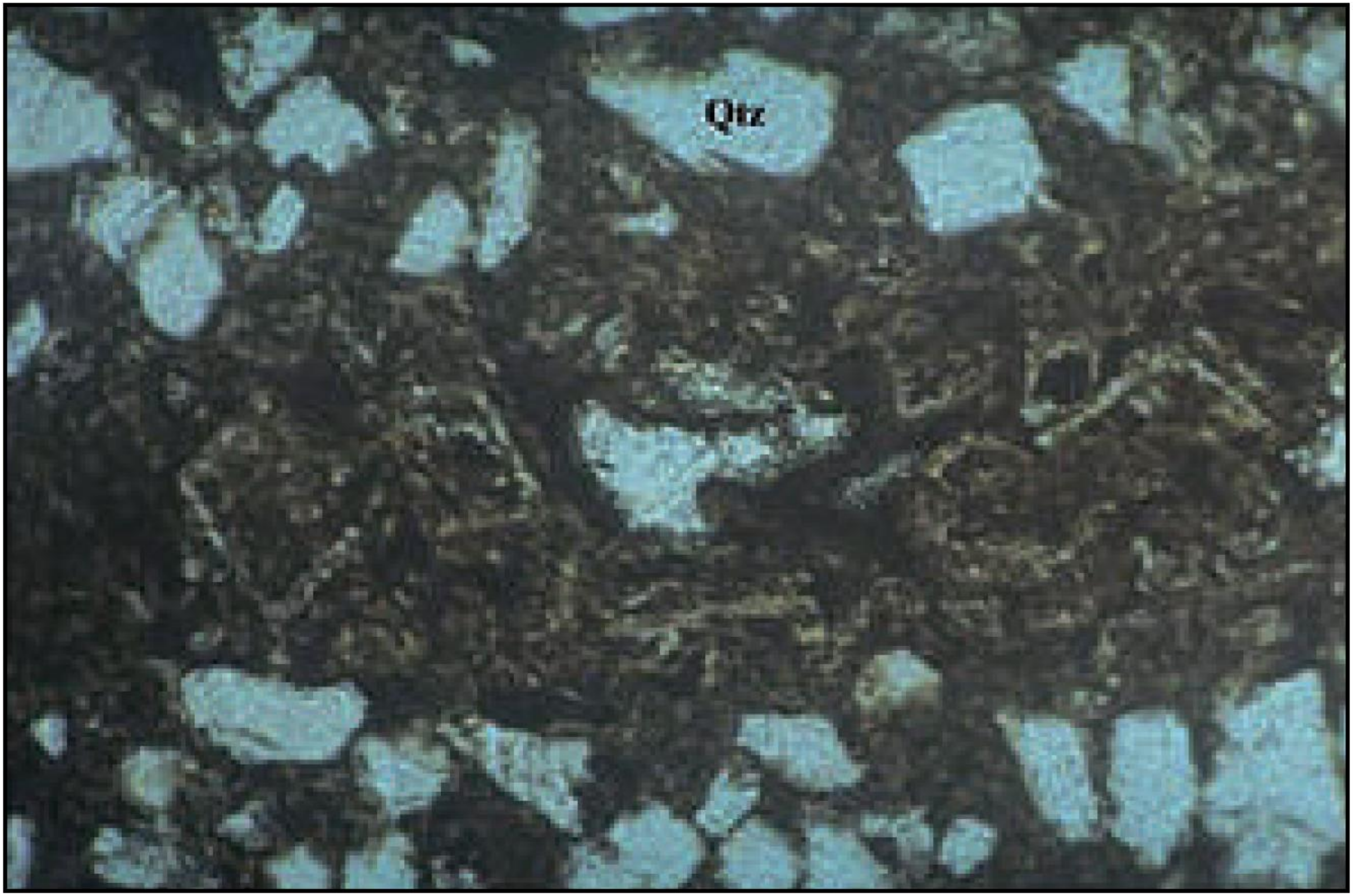

PM # 5. Sideritic cement, Sample No. 06, parallel nicols, 125X.

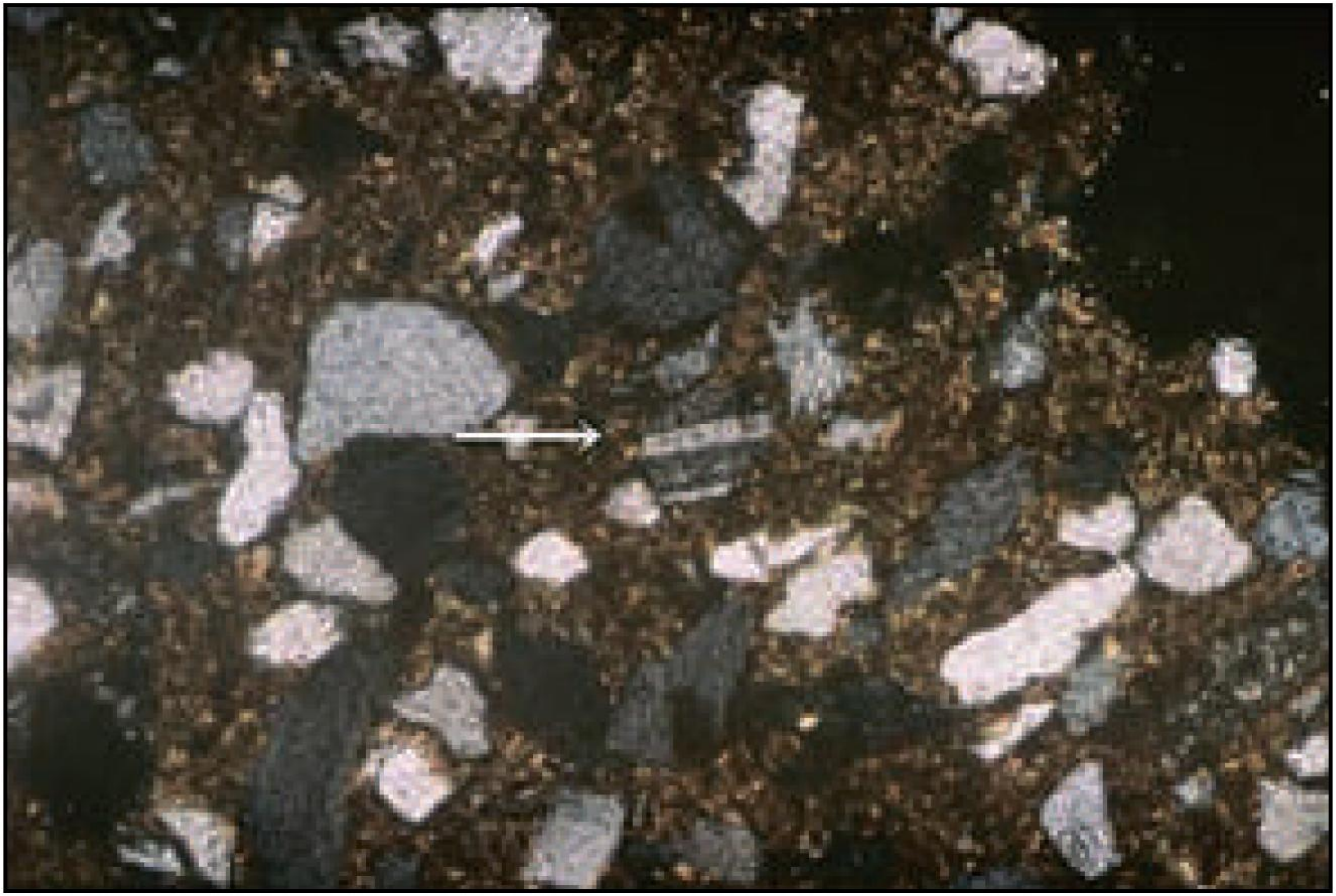

PM # 6. Rock fragment, Sample No. 06, cross nicols, 325X.

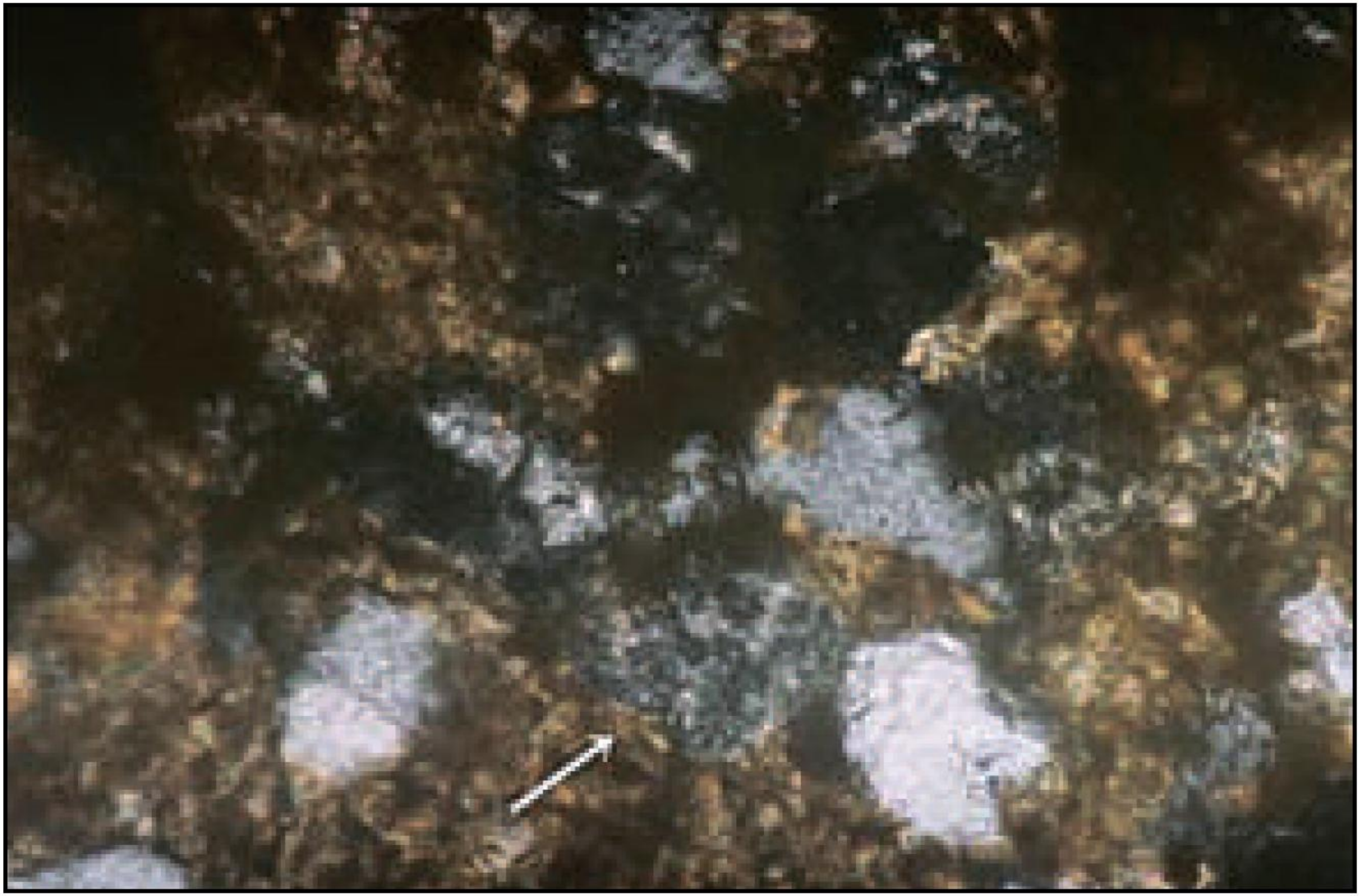

PM # 7. Rock fragment, Sample No. 06, cross nicols, 325X.

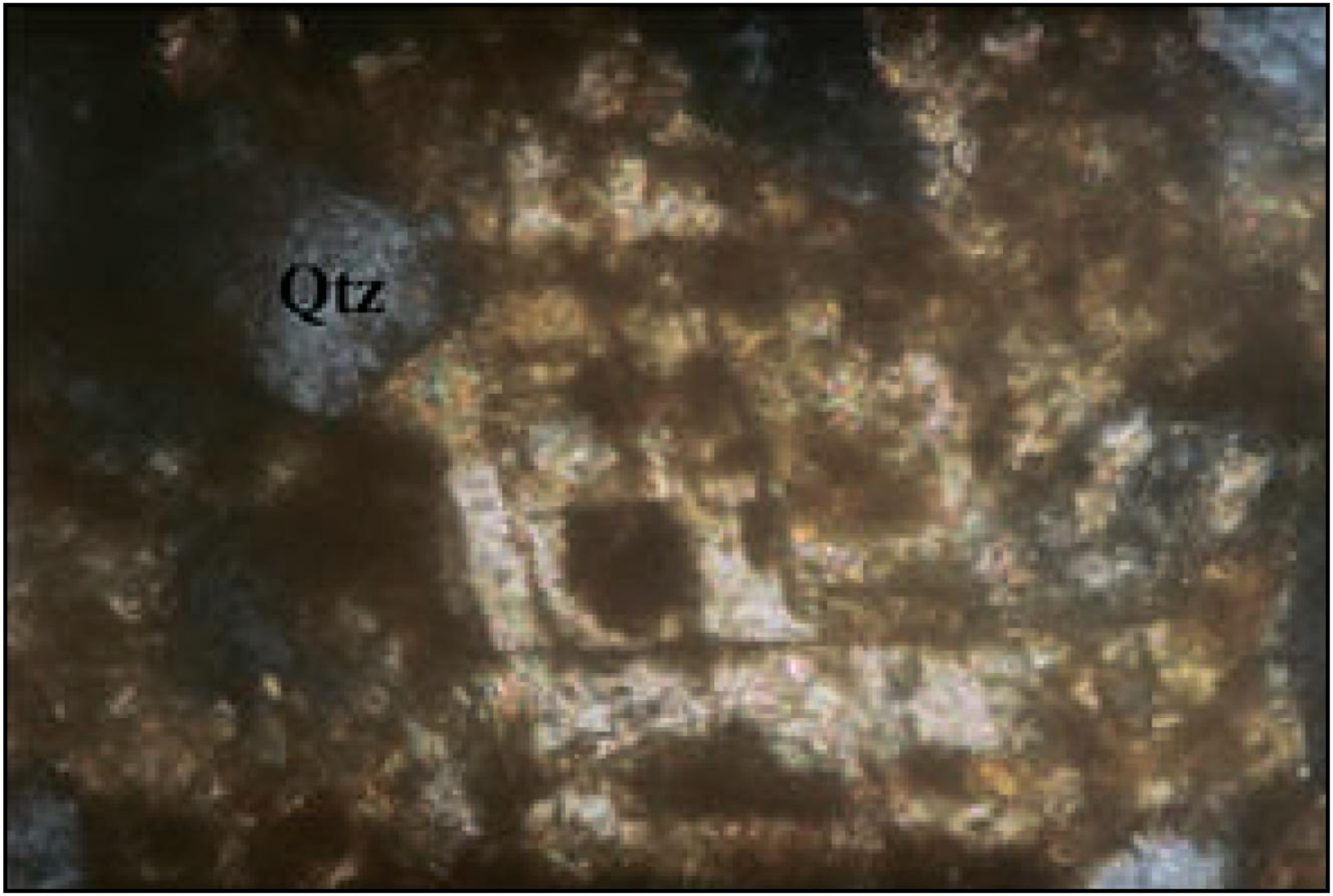

PM # 8. Siderite rhombs, Sample No. 06, cross nicols, 500X.

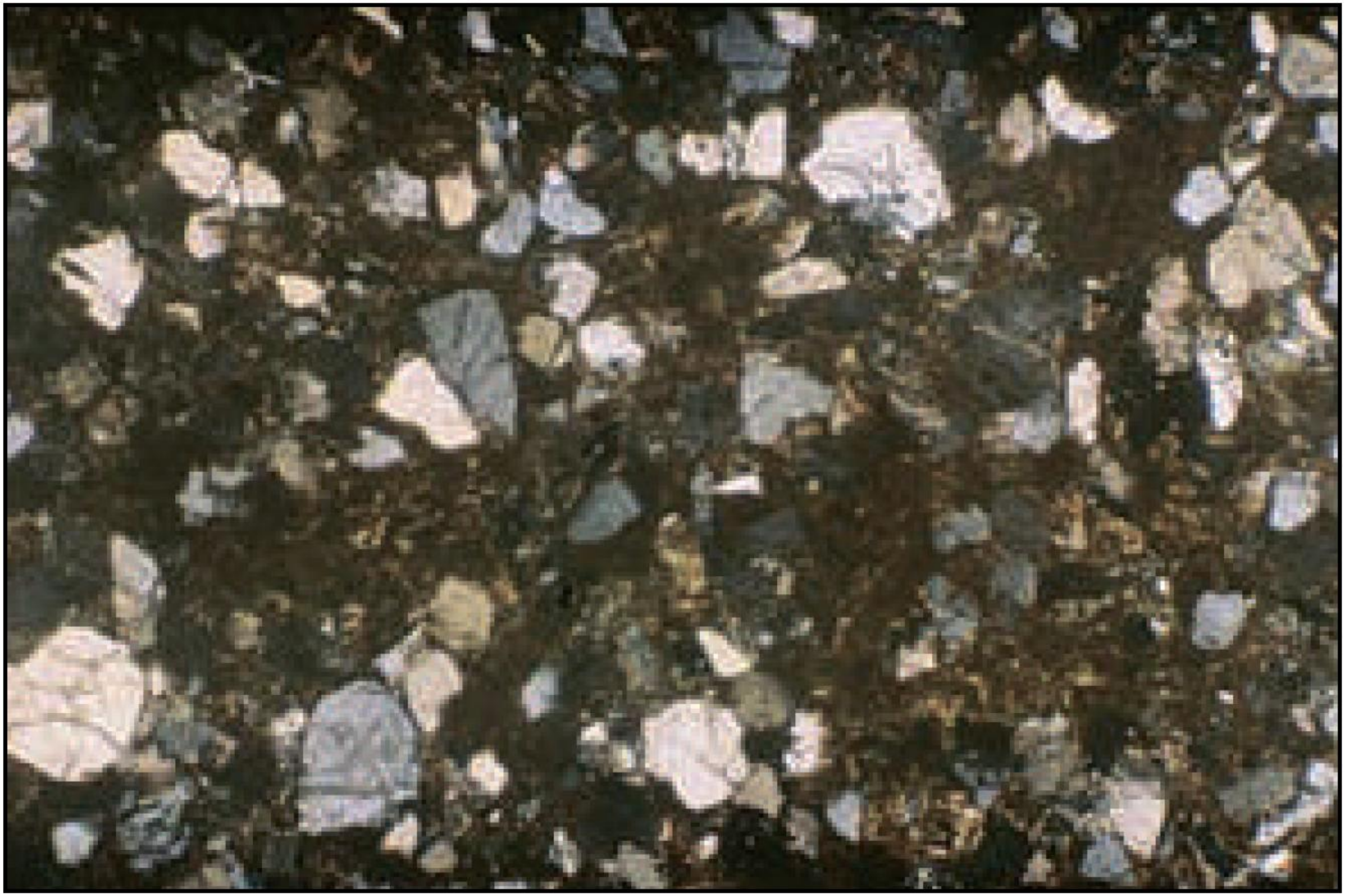

PM # 9. Bimodal nature, Sample No. 07, cross nicols, 50X.

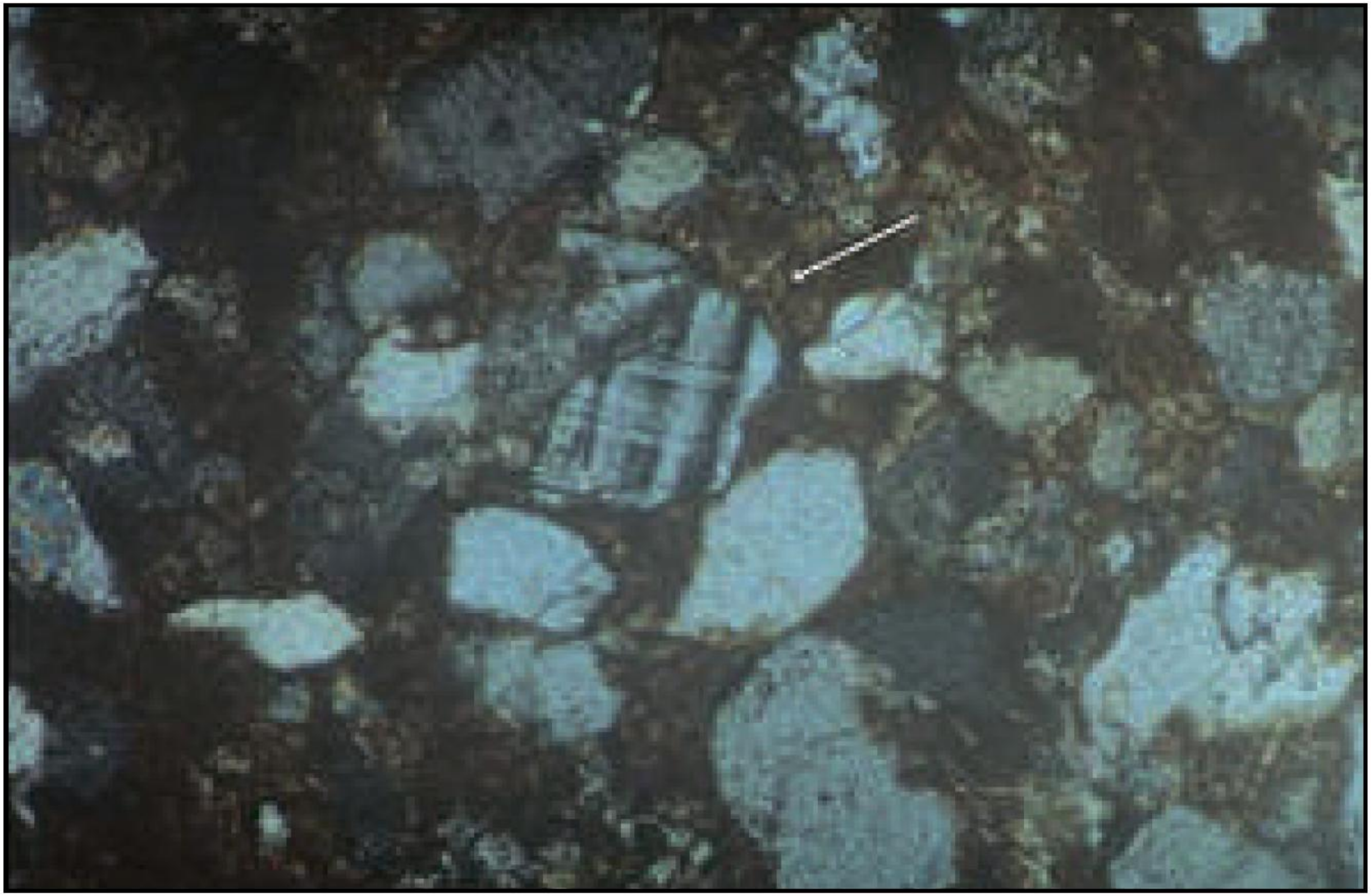

PM # 10. Microcline, Sample No. 07, cross nicols, 125X.

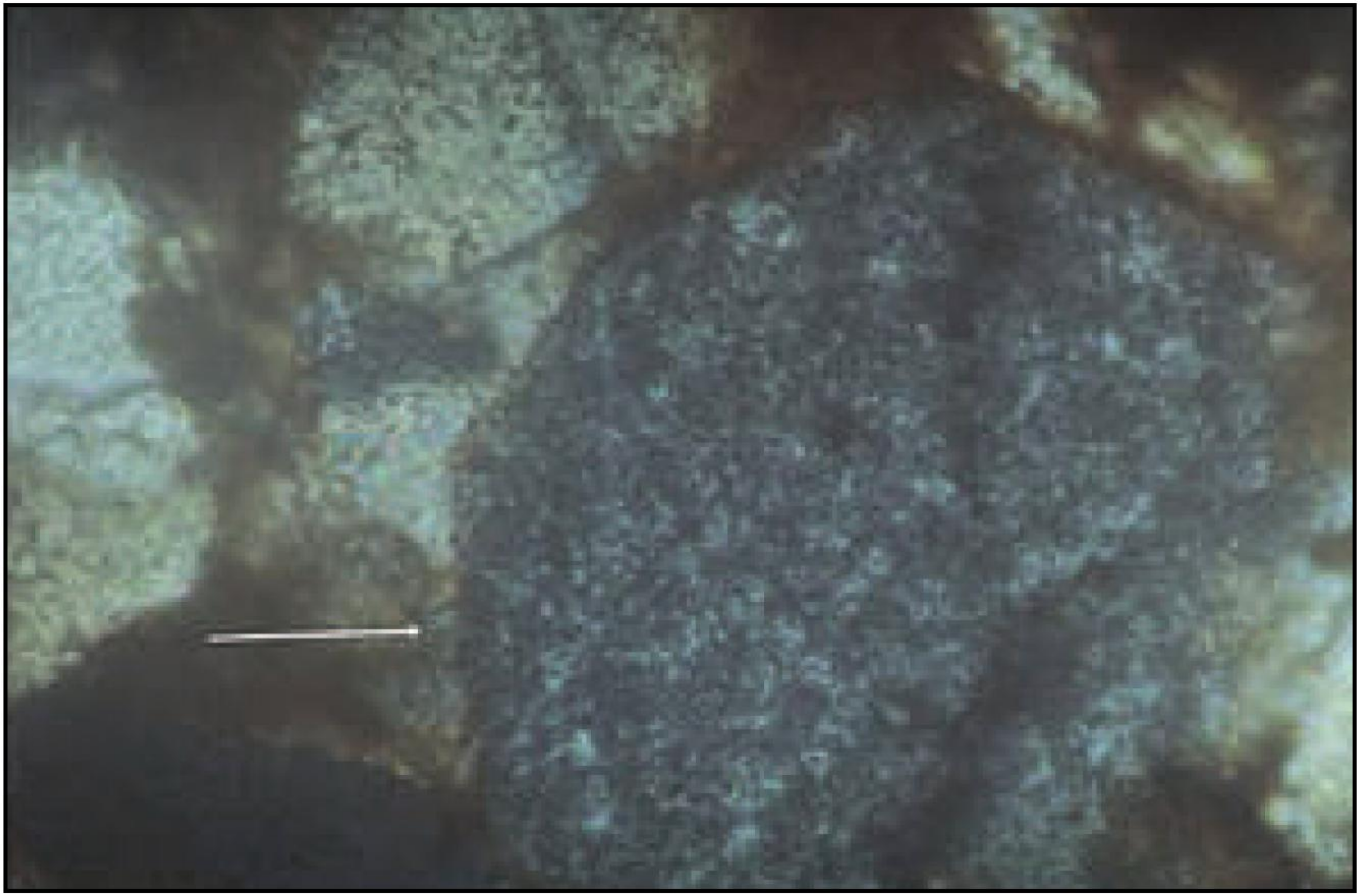

PM # 11. Rock fragment, Sample No. 07, cross nicols, 325X.

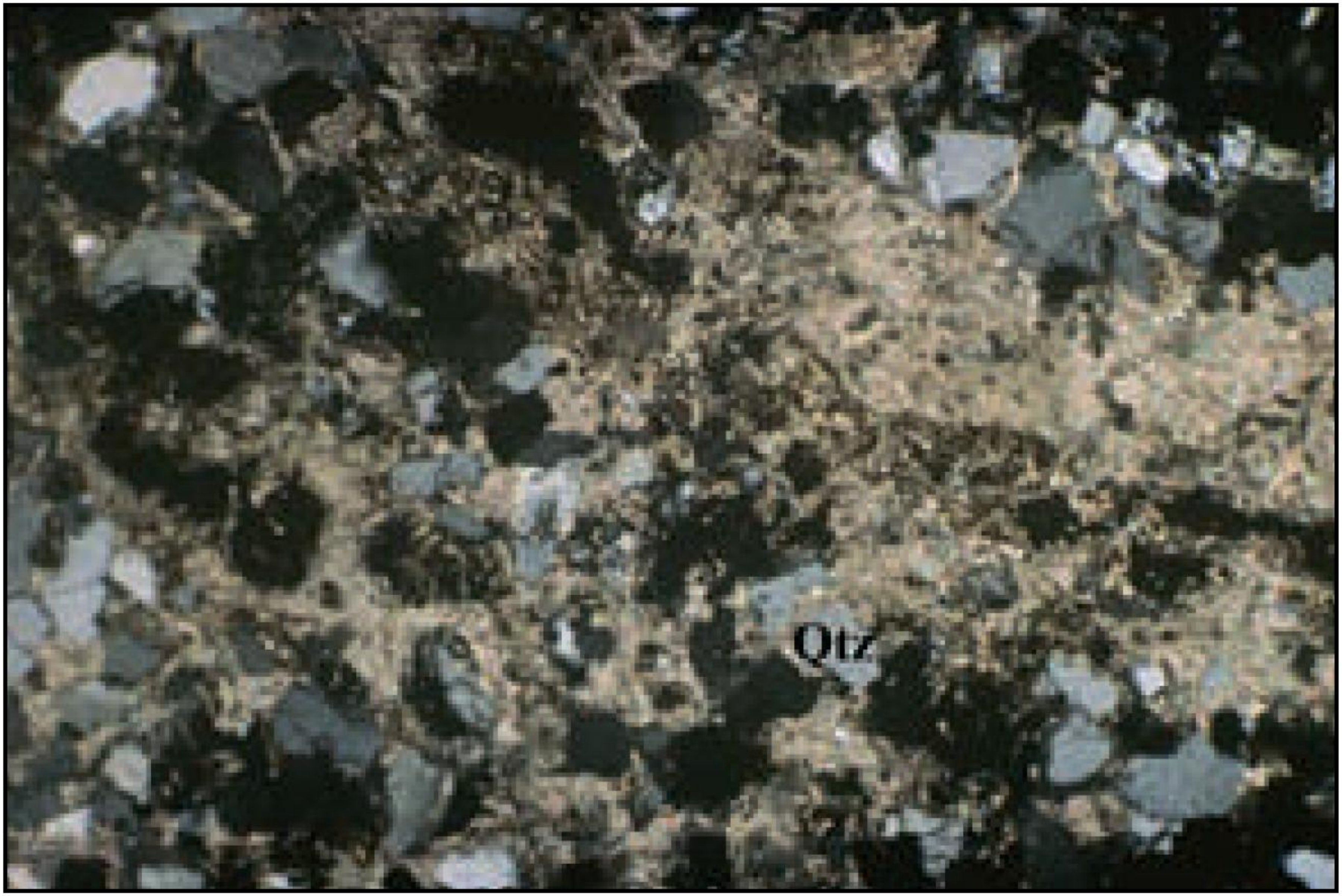

PM # 12. Calcareous cement, Sample No. 8L, cross nicols, 50X.

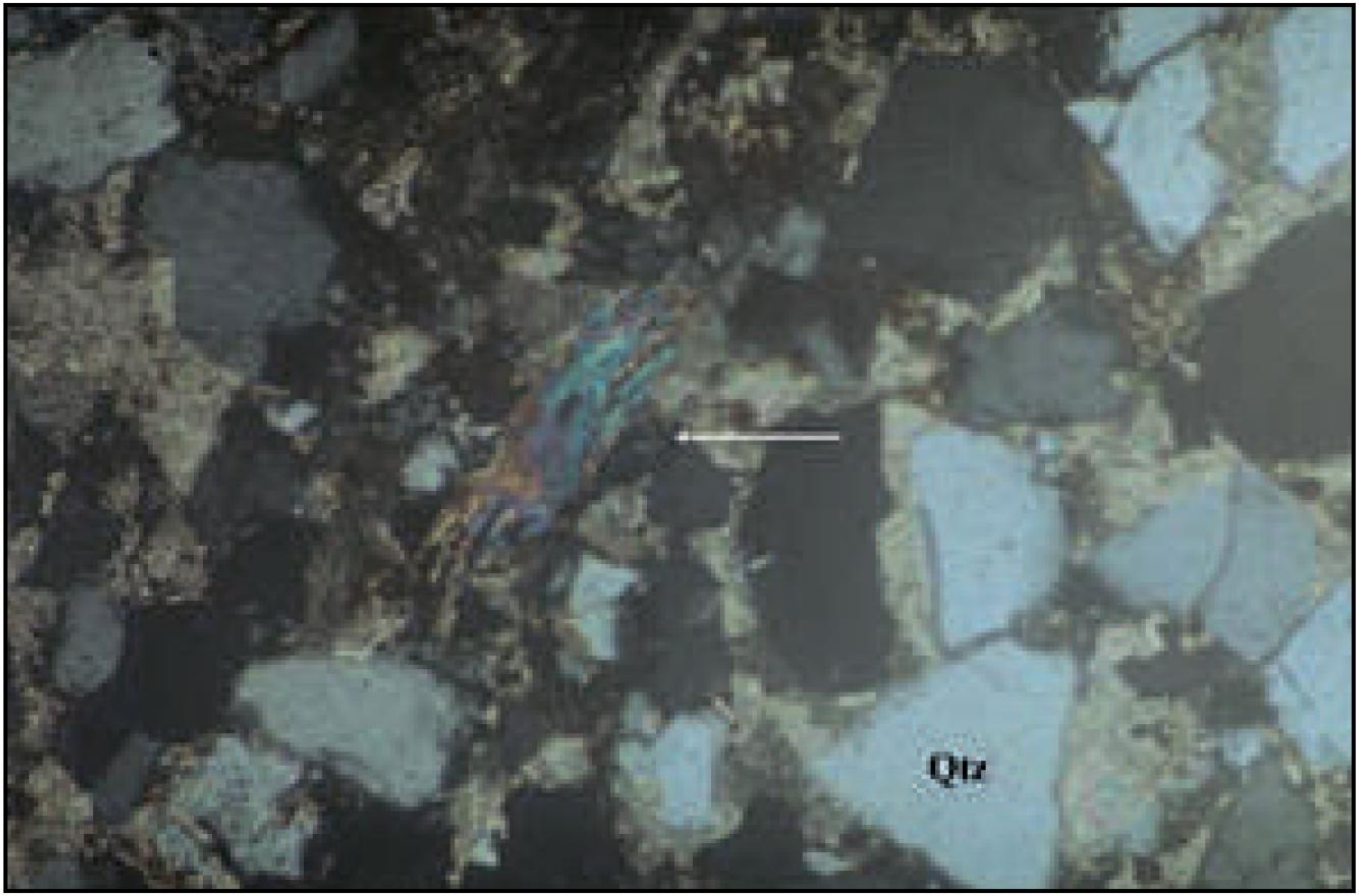

PM # 13. Muscovite, Sample No. 8L, cross nicols, 125X.

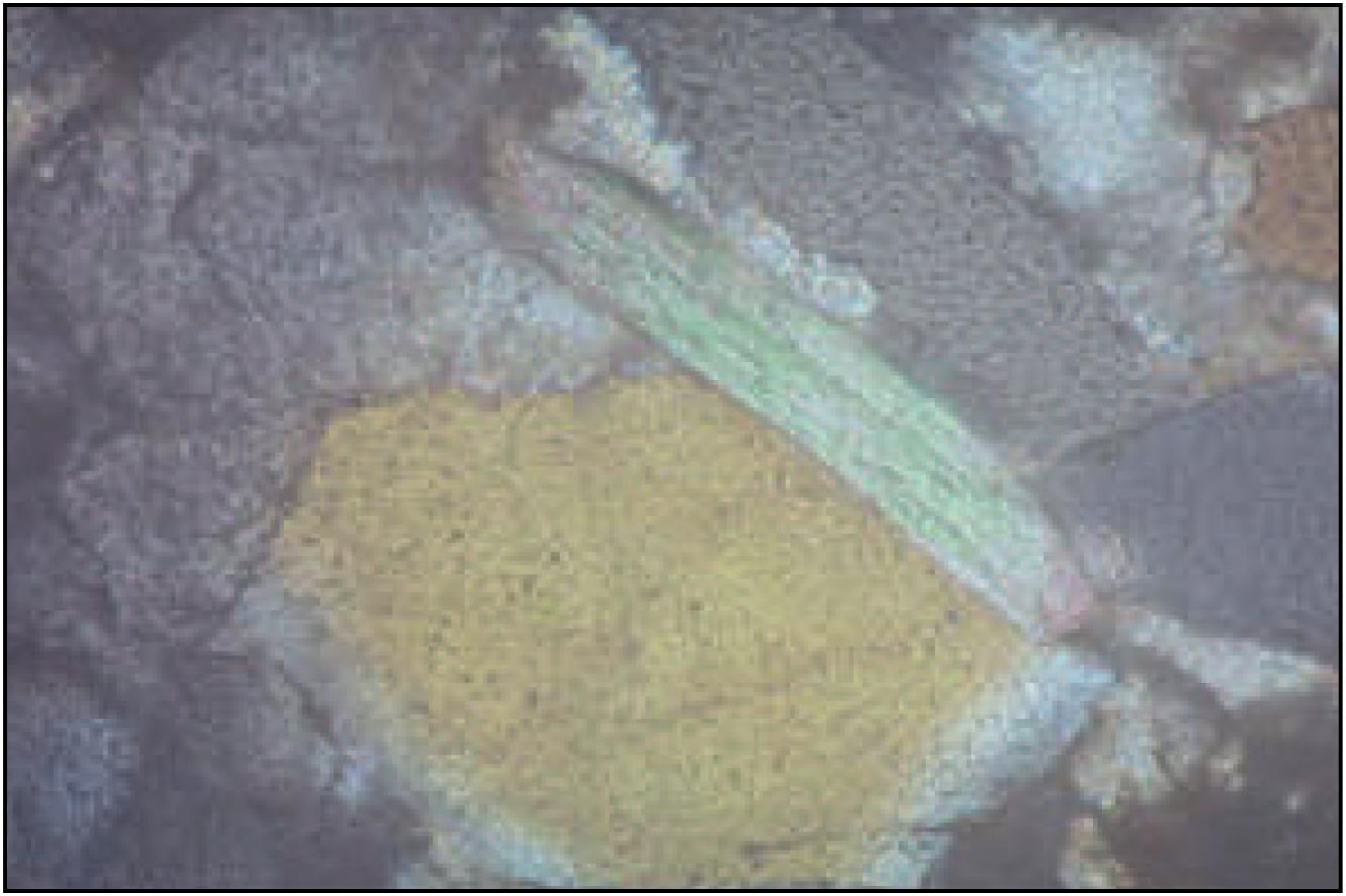

PM # 14. Muscovite, Sample No. 8L, cross nicols, 325X.

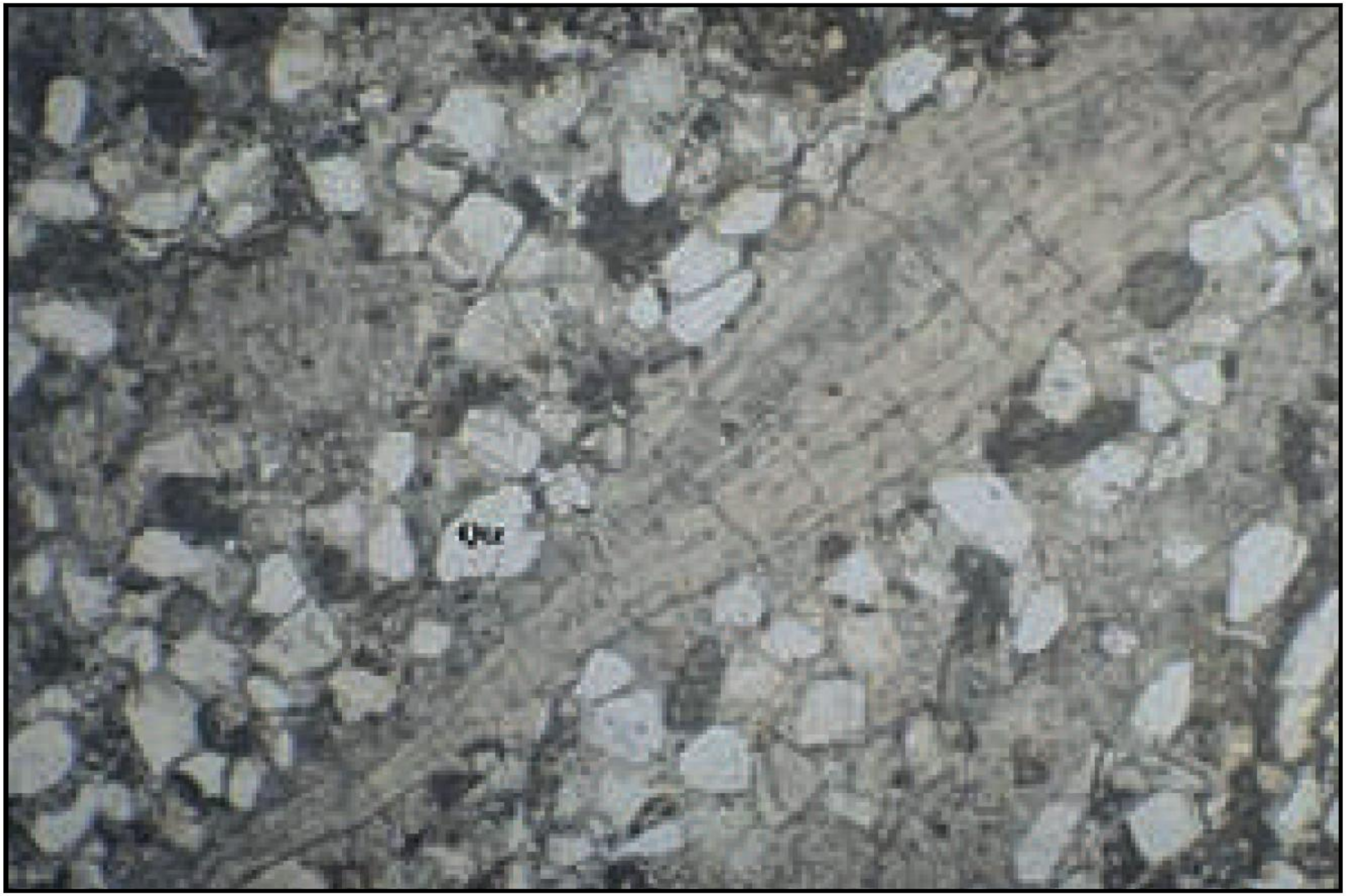

PM # 15. *Lepidocyclina*, Sample No. 8L, parallel nicols, 50X.

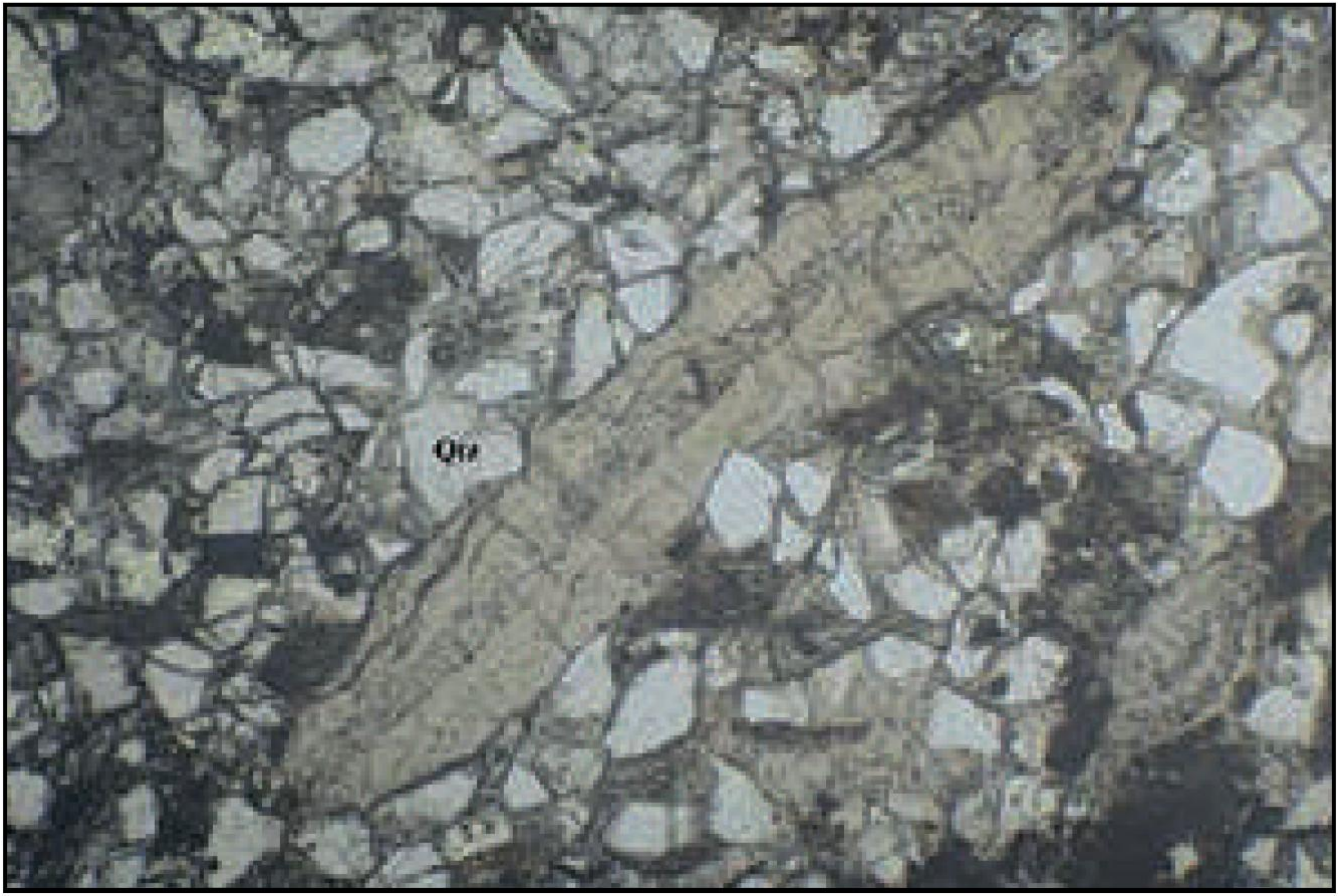

PM # 16. *Lepidocyclina polylepidine*, Sample No. 8L, parallel nicols, 50X.

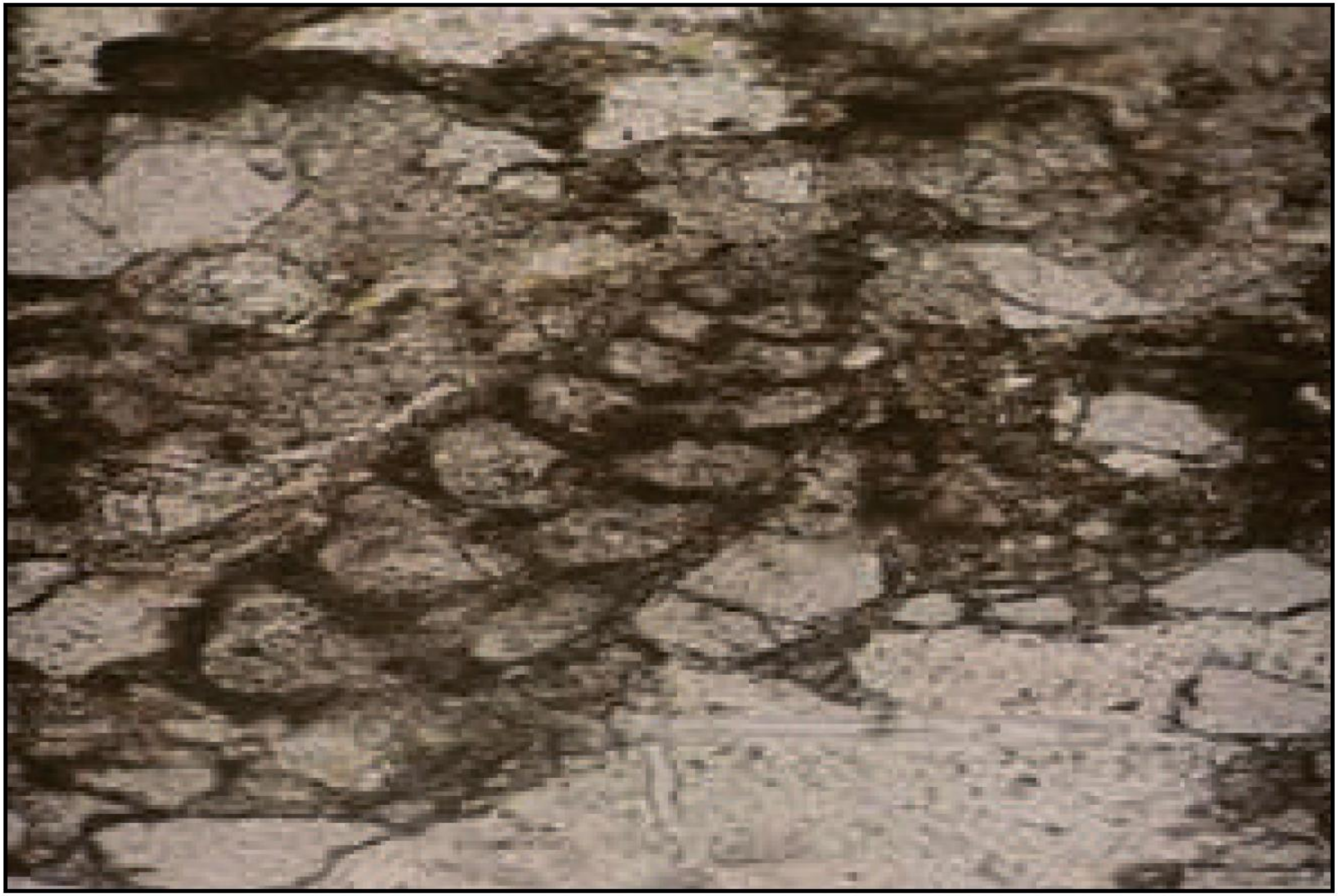

PM # 17. *Bermudizina*, Sample No. 8L, parallel nicols, 125X.

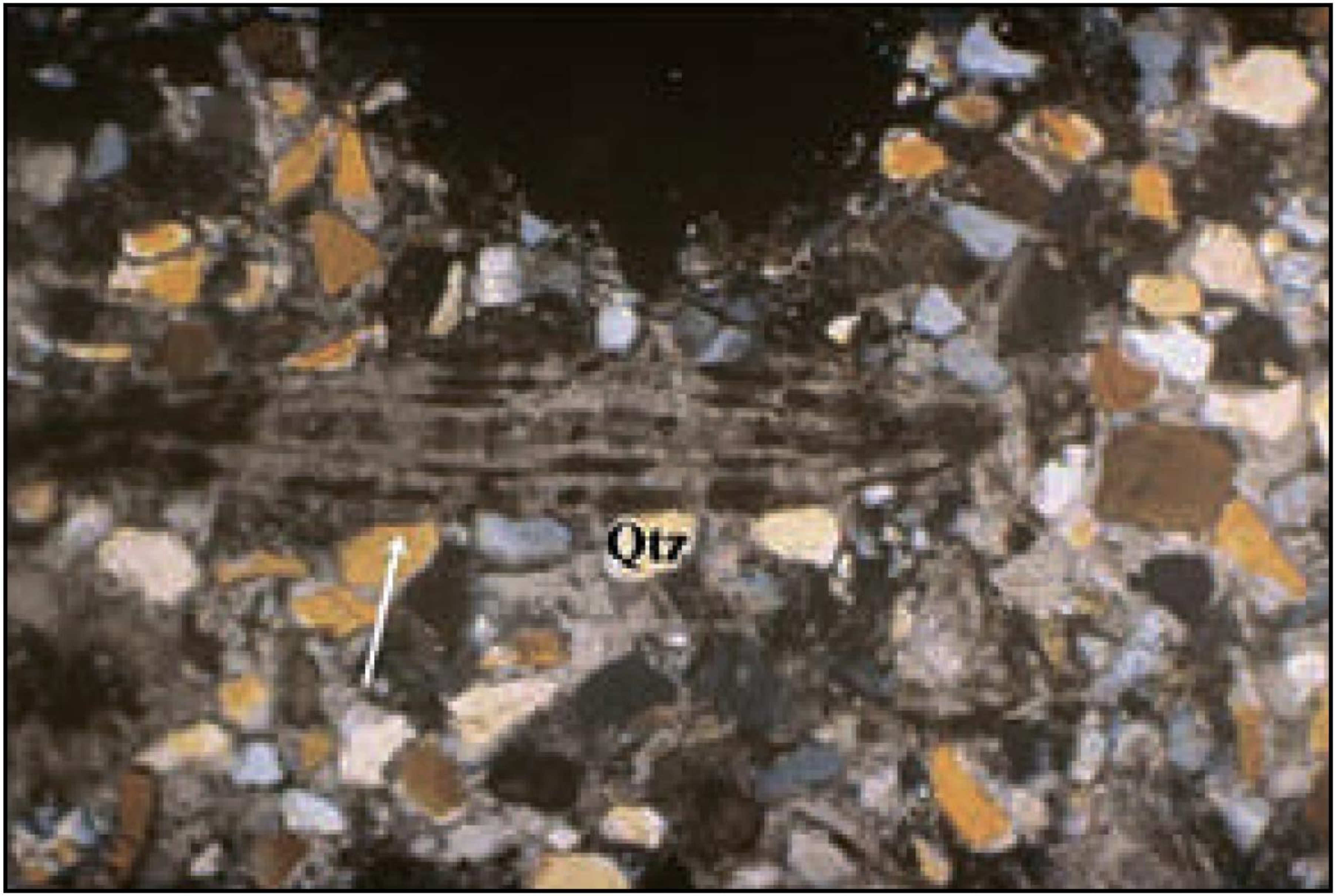

PM # 18. Fossil chamber filled with iron oxide, Sample No. 8L, cross nicols, 50X.

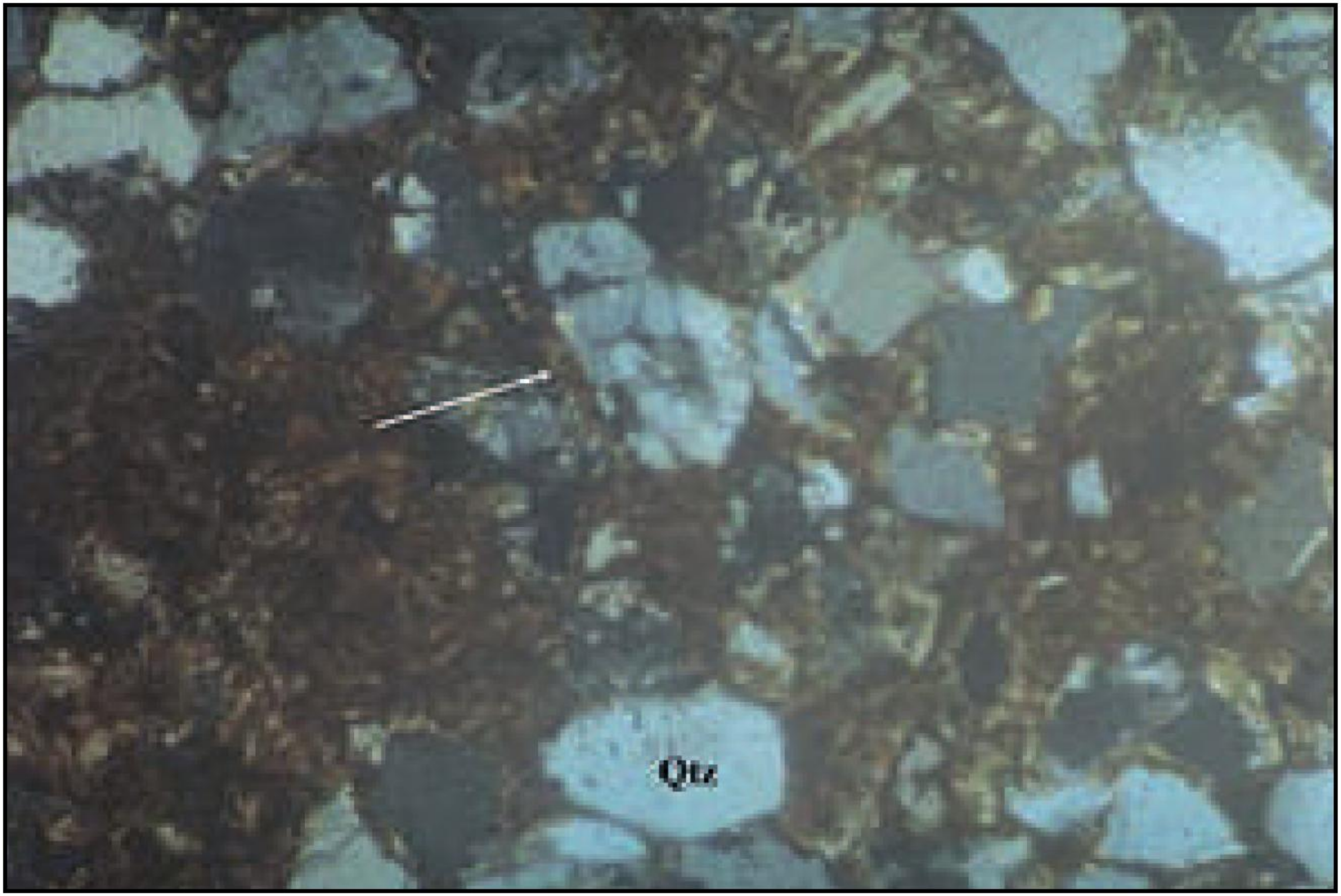

PM # 19. Polycrystalline quartz, Sample No. 8U, cross nicols, 125X.

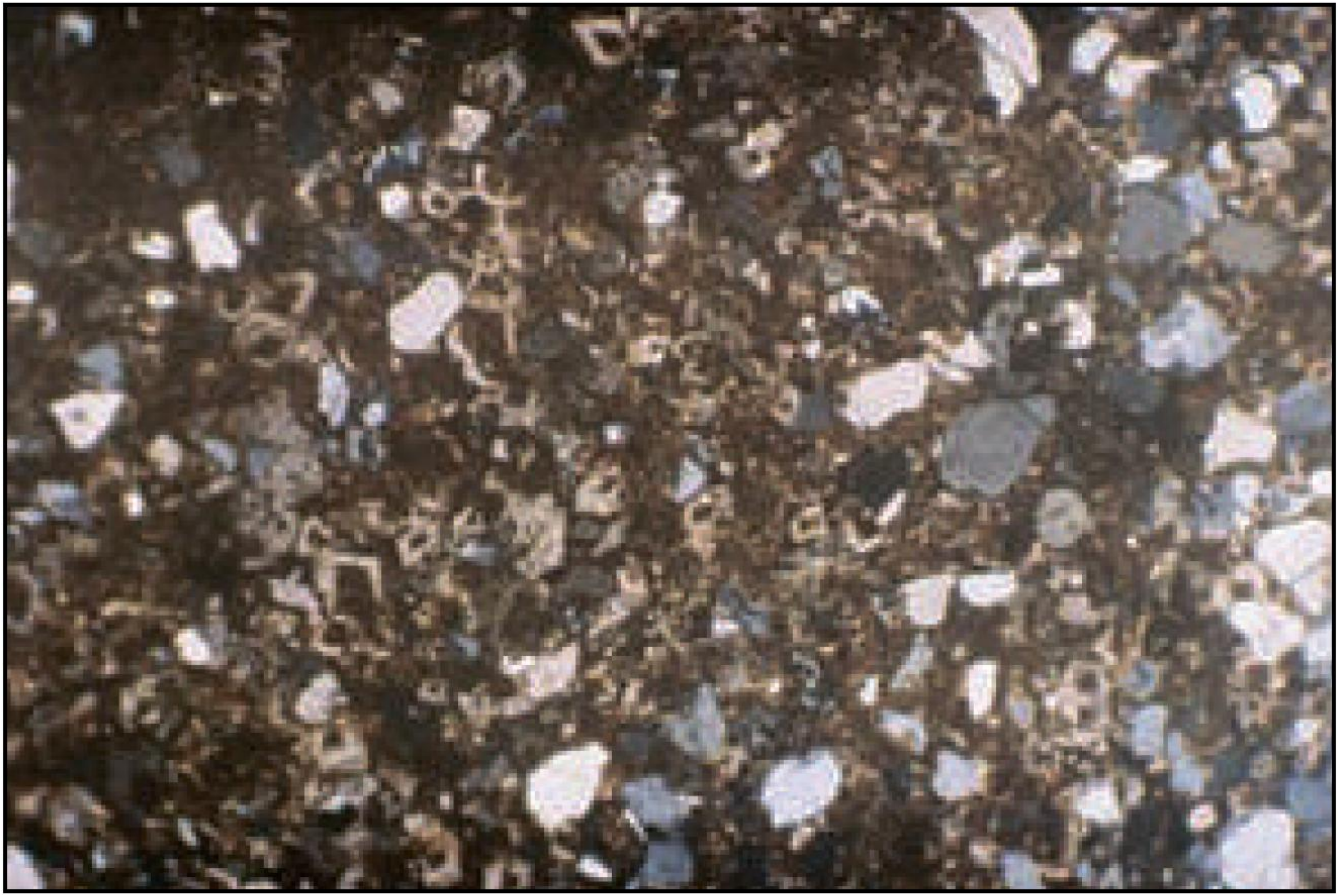

PM # 20. Zoned crystals of dolomite, Sample No. 8U, cross nicols, 50X.

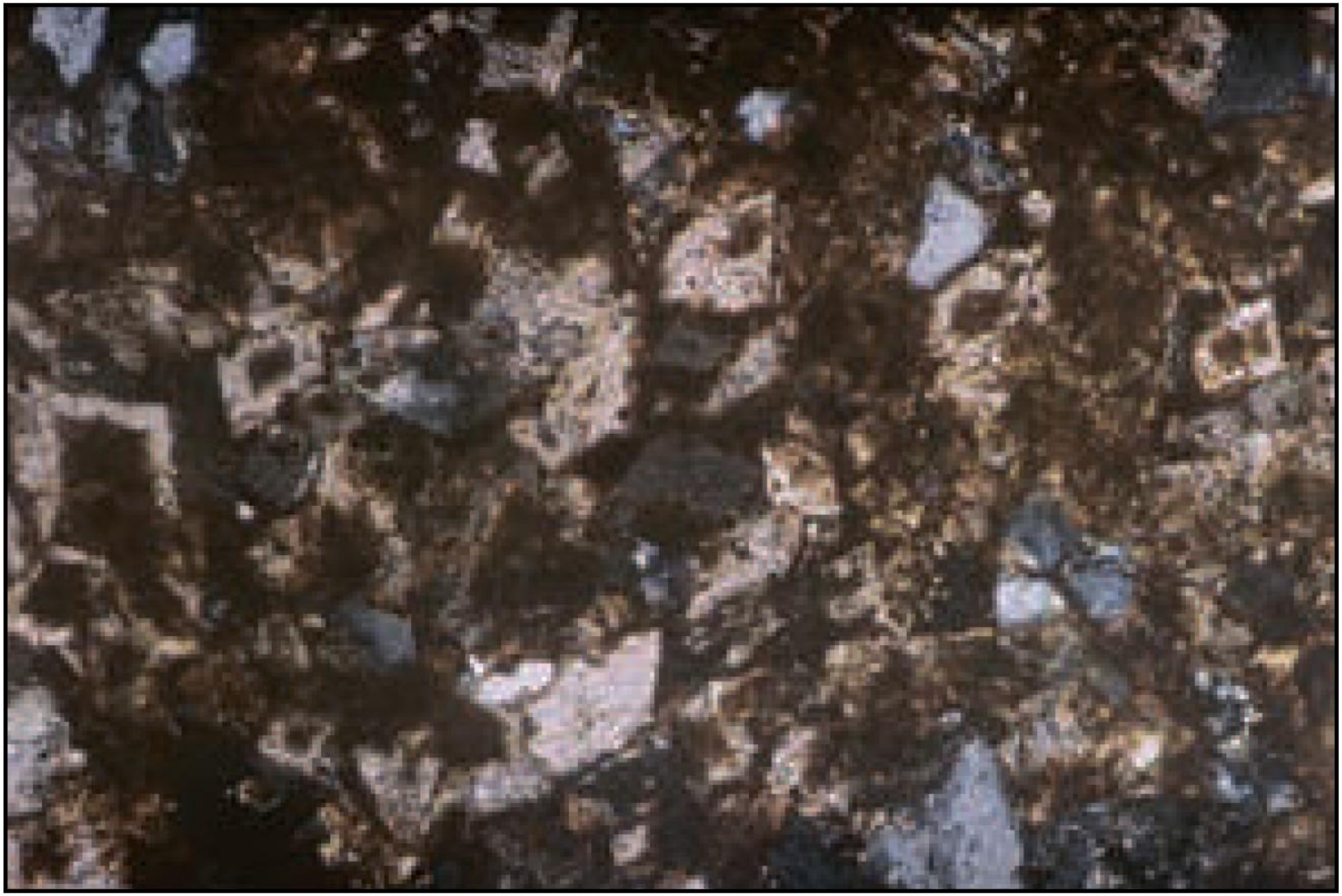

PM # 21. Zoned crystals of dolomite/siderite, Sample No.8U, cross nicols, 125X.